Interner Bericht
DESY-Zeuthen 96-04
Mai 1996

On Possible Future Polarized Nucleon–Nucleon Collisions at HERA

M.Anselmino, A.Jgoun, V.Korotkov, O.Martin,
F.Murgia, W.-D.Nowak, S.Nurushev, O.Teryaev, A.Tkabladze

Deutsches Elektronen-Synchrotron DESY
Institut für Hochenergiephysik IfH, Zeuthen
Platanenallee 6, D-15738 Zeuthen, Germany

"Die Verantwortung für den Inhalt dieses
Internen Berichtes liegt ausschließlich beim Verfasser"

Internal Report
DESY-Zeuthen 96-04
May 1996

On Possible Future Polarized Nucleon–Nucleon Collisions at HERA

M. Anselmino [1], A. Jgoun [2], V. Korotkov [3], O. Martin [4], F. Murgia [5], W.-D. Nowak [6], S. Nurushev [3], O. Teryaev [7], A. Tkabladze [7]

Abstract

The physics reach is investigated for polarized nucleon–nucleon collisions originating from an internal polarized target in the HERA proton beam. This study aims at finding boundary conditions for an upgraded or new spectrometer being able to measure single and – later, once the HERA proton beam should become polarized – double spin asymmetries in a fixed target environment at 40 GeV c.m. energy. Based on 240 pb^{-1} integrated luminosity, statistical sensitivities are given over a wide (x_F, p_T)–range for a variety of inclusive, semi–inclusive and elastic final states. By measuring single spin asymmetries essential conclusions can be drawn on the p_T-dependence of higher twist contributions. From double spin asymmetries it appears possible to measure the polarized gluon distribution in the range $0.1 \leq x_{gluon} \leq 0.4$ with good accuracy.

[1]University of Torino, Italy
[2]PNPI St. Petersburg, Russia
[3]IHEP Protvino, Russia
[4]University of Frankfurt, Germany
[5]University of Cagliari, Italy
[6]DESY-IfH Zeuthen, Germany
[7]JINR Dubna, Russia

1 Introduction

A complete theoretical picture of the nucleon structure will certainly have to incorporate the polarization degree of freedom, both in its perturbative and non-perturbative aspects. Although a largely consistent scheme exists since some time within the framework of perturbative Quantum Chromo Dynamics (pQCD) to describe short distance processes in strong interactions, the long distance sector of QCD is far from being fully understood even when appreciating the considerable progress made in recent lattice calculations (see e.g. [1]). Spin measurements have always been sources of unexpected surprises; the most recent example given by the simple and hitherto successful Quark Parton Model which could not describe the nucleon spin structure ('spin crisis') [2]. This caused a lot of theoretical papers and the recent next-to-leading order calculations [3] were found to reconcile the QCD improved Quark Parton Model with the results of the experiments. However, it is fair to say that the present knowledge of the polarized gluon distribution is still completely insufficient and the same applies to the polarized sea.

The spin crisis induced enormous theoretical and experimental activities. A number of new experiments was proposed to investigate in more detail the longitudinal spin structure of the nucleon by measuring double spin asymmetries in lepton nucleon collisions. Several measurements are already completed (E142 [4] and E143 [5] at SLAC) and some are still taking and/or analysing data (SMC [6] at CERN and E154 [7] at SLAC). Others have just started (HERMES [8] at DESY) or will start data taking soon (E155 [9] at SLAC). Nevertheless, it has to be mentioned that purely inclusive measurements determining the longitudinal spin structure functions $g_1(x, Q^2)$ for proton, neutron, and deuteron are unfortunately restricted to probe only certain combinations of the polarized valence, sea, and gluon contributions to the nucleon spin. A full analysis would require additional inputs from other measurements to separate the different components.

With the target polarization vector being oriented perpendicularly to the beam direction the transverse spin structure of the nucleon becomes accessible by measuring the spin structure functions $g_2(x, Q^2)$ which contain a twist–3 part that has recently been probed by SMC [10] and E143 [11], although still with large error bars. We note here that the underlying QCD correlators are at the same time describing the expected performance of single spin asymmetries measurable in nucleon–nucleon collisions [12].
Semi–inclusive measurements with SMC [13] and HERMES [8] will allow access to a variety of (combinations of) polarized parton distributions and to some polarized fragmentation functions. However, direct and separate measurements of the polarized gluon and sea quark distributions will remain of limited significance for quite some years.

A complementary window to study the nucleon spin structure will be opened once high energy polarized nucleon beams will become available with sufficiently high intensity. The only approved program up to now is the RHIC spin program [14] to be started early in the next millenium. As seen from today, no other comparable accelerator will be available at that time. Hence there is considerable interest in making HERA the second machine in the world offering two polarized high energy beams [15].

This paper intends to study in a first approximation the experimental possibilities when placing an internal polarized target into the (polarized) HERA proton ring. In principle

there exist three different future options to study polarized nucleon–nucleon interactions in fixed target mode at HERA. One obvious possibility would be to equip the future HERA West Hall experiment *HERA–B* [16] with a polarized internal target once the approved physics program be concluded. The spectrometer, under assembly at present, will have a rather large acceptance, a huge rate capability, and a quite complete particle identification system. Secondly, in the East Hall only about 40% of the floor is occupied by the *HERMES* experiment whose aperture poses, however, considerable constraints onto the nucleon–nucleon spin physics menu. Nevertheless, rotating the whole set–up by π and moving it into the proton beam line was kept as an option in the design from the beginning, although the high rate in the nucleon beam would require considerable upgrades. Last but not least the remaining free space in the East Hall could be used for a completely new experiment in the proton beam line which could be specifically designed according to the spin physics requirements. However, at the moment any site discussion appears premature and hence this study aims at being as much as possible independent of a final site decision. For the sake of simplicity the envisaged spin physics experiment will be called *HERA–$\vec{N}$* throughout this paper.

2 Polarized Nucleon–Nucleon Physics at HERA

An experiment utilising an internal polarized nucleon target in the 820 GeV HERA proton beam would constitute a logical extension of studying at DESY the nucleon structure in more detail by investigating its spin degrees of freedom, as it commenced with the *HERMES* experiment. Judged from today, this would be the only other place to study high energy nucleon–nucleon spin physics besides the envisaged dedicated RHIC spin program at BNL which is supposed to get started in about five years from now.
An internal polarized nucleon target offers unique features such as polarization above 80%, no or small dilution, and a high density up to 10^{14} atoms/cm^2 [17]. Moreover, rather small systematic errors are expected when comparing proton and neutron results obtained from Hydrogen and Deuterium gas data, respectively.
As long as the polarized target is operated in the unpolarized proton beam, the physics scope of *HERA–$\vec{N}$* would be focused to 'phase I', i.e. measurements of single spin asymmetries [18, 19, 20]. Once later polarized protons should become available, the same set-up would be readily available to measure various kinds of double spin asymmetries. These 'phase II' measurements would constitute an alternative – fixed target – approach to similar physics as it will be accessible to the collider experiments *STAR* and *PHENIX* at the low end of the RHIC energy scale ($\sqrt{s} \simeq 50$ GeV) [21].

Single Spin Asymmetries

Single spin asymmetries in large p_T inclusive production, both in proton-nucleon and lepton-nucleon interactions, have recently received much attention [22]-[40]. The naive expectation that they should be zero in perturbative QCD has been proven to be false, both experimentally [19, 23, 25] and theoretically [30]-[34]. It is now clear that higher twist effects are responsible for these asymmetries, which should be zero only in leading twist-2 perturbative QCD.
Several models and theoretical analyses suggest possible higher twist effects: there might be twist-3 dynamical contributions, which we shall denote as hard scattering higher twists

[35]; there might also be intrinsic $k_\perp$ effects, both in the quark fragmentation process [29, 31] and in the quark distribution functions [26, 27, 32, 34]. The latter are not by themselves higher twist contributions - they are rather non-perturbative universal nucleon properties - but give rise to twist-3 contributions when convoluted with the hard scattering cross sections.
The dynamical contributions result from a short distance part calculable in perturbative QCD with slightly modified Feynman rules, combined with a long distance part related to quark-gluon correlations [35].
An intrinsic $k_\perp$ effect in the quark fragmentation has been first introduced in Ref. [29] and is known as Collins or sheared jet effect; it simply amounts to say that the number of hadrons h (say, pions) resulting from the fragmentation of a transversely polarized quark, with longitudinal momentum fraction z and transverse momentum $\boldsymbol{k}_\perp$, depends on the quark spin orientation. That is, one expects

$$D_{h/q^\uparrow}(z, \boldsymbol{k}_\perp) \neq D_{h/q^\downarrow}(z, \boldsymbol{k}_\perp)\,, \tag{1}$$

where, by parity invariance, the quark spin should be orthogonal to the $q - h$ plane. Notice also that time reversal invariance does not forbid such quantity to be $\neq 0$ because of the (necessary) soft interactions of the fragmenting quark with external strong fields, i.e. because of final state interactions. Eq. (1) implies that the *quark fragmentation analysing power* $A_q(\boldsymbol{k}_\perp)$ can be different from zero:

$$A_q(\boldsymbol{k}_\perp) \equiv \frac{D_{h/q^\uparrow}(z, \boldsymbol{k}_\perp) - D_{h/q^\downarrow}(z, \boldsymbol{k}_\perp)}{D_{h/q^\uparrow}(z, \boldsymbol{k}_\perp) + D_{h/q^\downarrow}(z, \boldsymbol{k}_\perp)} \neq 0 \tag{2}$$

This idea has been applied to the computation of the single spin asymmetries observed in $pp^\uparrow \to \pi X$ [31].
A similar idea applies to the distribution functions, provided soft gluon interactions between initial state partons are present and taken into account, which most certainly is the case for hadron-hadron interactions [26, 27, 32, 34]. That is, one can expect that the number of quarks with longitudinal momentum fraction x and transverse intrinsic motion $\boldsymbol{k}_\perp$ depends on the transerve spin direction of the parent nucleon:

$$f_{q/N^\uparrow}(x, \boldsymbol{k}_\perp) \neq f_{q/N^\downarrow}(x, \boldsymbol{k}_\perp) \tag{3}$$

Eq. (3) implies that the *quark distribution analysing power* $N_q(\boldsymbol{k}_\perp)$ can be different from zero:

$$N_q(\boldsymbol{k}_\perp) \equiv \frac{f_{q/N^\uparrow}(x, \boldsymbol{k}_\perp) - f_{q/N^\downarrow}(x, \boldsymbol{k}_\perp)}{f_{q/N^\uparrow}(x, \boldsymbol{k}_\perp) + f_{q/N^\downarrow}(x, \boldsymbol{k}_\perp)} \neq 0 \tag{4}$$

This effect also has been used to explain the single spin asymmetries observed in $pp^\uparrow \to \pi X$ [32, 34]. Let us notice again that both $A_q(\boldsymbol{k}_\perp)$ and $N_q(\boldsymbol{k}_\perp)$, Eqs. (2) and (4) respectively, are leading twist quantities, which, when convoluted with the elementary cross-sections and integrated over $\boldsymbol{k}_\perp$, give twist-3 contributions to the single spin asymmetries [31, 34].
Each of the above mechanisms might be present and might be important in understanding twist-3 contributions; in particular the quark fragmentation or distribution analysing powers look like new non-perturbative universal quantities, crucial in clarifying the spin structure of nucleons. It is then of great importance to study possible ways of disentangling these different contributions in order to be able to assess the importance of each of them.

We propose here several different processes and measurements which should allow to fulfill such a task. For the sake of completeness we not only consider nucleon-nucleon interactions but also other processes, like lepton-nucleon scattering, which might add valuable information.
Let us then consider several processes $A + B^{\uparrow} \to C + X$ and the related single spin asymmetries

$$\frac{d\sigma^{AB^{\uparrow}\to CX} - d\sigma^{AB^{\downarrow}\to CX}}{d\sigma^{AB^{\uparrow}\to CX} + d\sigma^{AB^{\downarrow}\to CX}}; \tag{5}$$

for each of them we discuss the possible sources of higher twist contributions, distinguishing, according to the above discussion, between those originating from the hard scattering and those originating either from the quark fragmentation or distribution analysing power.

- $pN^{\uparrow} \to hX$

In this process all kinds of higher twist contributions may be present; those related to $k_{\perp}$ effects in the fragmentation function have been considered in Ref. [31] and those related to $k_{\perp}$ effects in the distribution function in Refs. [32, 34]. This asymmetry *alone* could not help in evaluating the relative importance of the different terms.

- $pN^{\uparrow} \to \gamma X$ or $pN^{\uparrow} \to \mu^{+}\mu^{-}X$

Here there is no fragmentation process, and we remain with possible sources of non-zero single spin asymmetries in the hard scattering or the quark distribution analysing power.

- $lN^{\uparrow} \to hX$

In such a process the single spin asymmetry can originate either from hard scattering or from $k_{\perp}$ effects in the fragmentation function, but not in the distribution functions, as soft initial state interactions are suppressed by powers of α_{em}. Moreover, this process allows, in principle, a direct measurement of the Collins effect, i.e. of the quark fragmentation analysing power, via a measurement of the leading-twist difference of cross sections for the production of two identical particles inside the same jet, with opposite $\boldsymbol{k}_{\perp}$:

$$\frac{E_h d\sigma^{lN^{\uparrow}\to hX}}{d^3p_h d^2k_{\perp}}(\boldsymbol{p}_h = z\boldsymbol{p}_q + \boldsymbol{k}_{\perp}) - \frac{E_h d\sigma^{lN^{\uparrow}\to hX}}{d^3p_h d^2k_{\perp}}(\boldsymbol{p}_h = z\boldsymbol{p}_q - \boldsymbol{k}_{\perp}) \tag{6}$$

which is proportional to Eq. (2).

- $lp^{\uparrow} \to \gamma X$, $\gamma p^{\uparrow} \to \gamma X$, $lp^{\uparrow} \to \mu^{+}\mu^{-}X$

Each of these processes yields a single spin asymmetry which cannot originate from distribution or fragmentation $\boldsymbol{k}_{\perp}$ effects; it may only be due to higher-twist hard scattering effects, which would thus be isolated.

It is clear from the above discussion that a careful and complete study of single spin asymmetries in several processes might be a unique way of understanding the origin and importance of higher twist contributions in inclusive hadronic interactions; not only, but it might also allow a determination of fundamental non-perturbative properties of quarks inside polarized nucleons and of polarized quark fragmentations. Such properties should be of universal value and applicability and their knowledge might be as important as the knowledge of unpolarized distribution and fragmentation functions. In section 5 we

shall discuss in more detail some of the processes proposed here; there it will be shown that within the given kinematical situation at HERA from measurements of single spin asymmetries conclusive information can be drawn about the validity of the spin sector of Quantum Chromo Dynamics in general, and about the onset of its perturbative regime in particular.

Double Spin Asymmetries.

Perturbative QCD allows for a simple calculation of Born double spin asymmetries for various 2→2 subprocesses at the partonic level. The one-loop radiative corrections to various subprocesses have been calculated [41], showing only small changes in the asymmetry in comparison with leading order. Relying on factorization a rich spectrum of hadronic level asymmetries can be predicted which constitutes the backbone of the RHIC spin physics program [42, 43]. When both incoming particles are longitudinally polarized, the above discussed insufficient knowledge of the polarized gluon distribution makes the predictions for double spin asymmetries A_{LL} to some extent uncertain. Conversely, the measurement of A_{LL} in certain final states (e.g. photon plus jet) is presently considered to be the most reliable method to measure the polarized gluon distribution. In a similar way the dilepton final state might be used to accomplish a separate measurement of the polarized sea when orienting both incoming polarizations transversely. In this configuration access is possible to the hitherto totally unmeasured twist–2 transverse spin structure function $h_1(x)$ which is totally inaccessible in inclusive lepton–nucleon deep inelastic scattering due to an additional suppression factor. Some first data on $h_1(x)$ might be obtained from semi–inclusive pion asymmetries [44], as it is envisaged by the HERMES experiment.
In the following some first estimates will be given on the sensitivity of $HERA$–$\vec{N}$ in doubly polarized mode ('Phase II') to measure the polarized gluon distribution.

3 Luminosity, Sensitivity, Acceptance, Rate

The experimental sensitivity in measuring a spin asymmetry A is given by [45]

$$\delta A = \frac{1}{P_B \cdot P_T} \cdot \frac{1}{\sqrt{C \cdot \mathcal{L} \cdot T}} \cdot \frac{1}{\sqrt{\sigma}} ,$$

where P_B and P_T are the average beam and target polarisation, respectively. Throughout the paper $P_B = 0.6$ and $P_T = 0.8$ are assumed. The beam polarization is taken as unity when single spin asymmetries are considered. $C \simeq 50\%$ represents the anticipated combined trigger and reconstruction efficiency and σ is the unpolarized cross-section.
Using $\bar{I}_B = 80$ mA $= 0.5 \cdot 10^{18}\ s^{-1}$ as a realistic figure for the 1996 average HERA proton beam current and a realistic polarized target density of $n_T = 3 \cdot 10^{13}$ atoms/cm^2 [17] the projected luminosity becomes

$$\mathcal{L} = n_T \cdot \bar{I}_B = 1.5 \cdot 10^{31}\ \mathrm{cm}^{-2} s^{-1} .$$

For the total running time T an equivalent of $T = 1.6 \cdot 10^7\ s$ at 100 % efficiency is assumed. Under 1995 realistic HERA conditions with 33% combined up–time for accelerator and experiment this corresponds to about 3 calendar years of machine operation with 6 months physics running per year.

The integrated luminosity is then obtained as

$$\mathcal{L} \cdot T = 240\ pb^{-1}$$

Finally, the projected sensitivities are given by

$$\delta A_{ssa} = 0.10/\sqrt{\sigma/[pb]} \quad \text{for single spin asymmetries and}$$
$$\delta A_{dsa} = 0.17/\sqrt{\sigma/[pb]} \quad \text{for double spin asymmetries.}$$

Experience from UA6 running at CERN indicates that after having gained some practical running experience it might turn out being feasible to operate the polarized gas target at a 2 or 3 times higher density without seriously affecting the proton beam lifetime. In addition, proton currents much higher than the original HERA design value of 160 mA might be provided later in a possible HERA high luminosity scenario. Hence in a few years 500 pb^{-1} per year might become a realistic figure.

Generally speaking, the loss in acceptance for a typical fixed target spectrometer amounts to about $\frac{2}{3}$, caused by the usually incomplete azimuthal coverage. Not to restrict the discussion too early to a special scenario, however, we disregard at the present level of accuracy any detector acceptance with some exceptions in case of jet detection. In addition we note that in the cross section calculation for single spin asymmetries enters the scalar product between the pseudovector normal to the scattering plane and the target polarization vector. The latter being oriented vertically single spin asymmetries are preferentially to be measured as left–right counting rate asymmetries. For a typical apparatus preferring the horizontal over the vertical aperture this additional loss in acceptance is small and will be neglected at present.

Summarizing the luminosity and acceptance estimates on the present level of investigations we conclude as follows. On one hand, any realistic spectrometer acceptance will decrease all sensitivities by about $1/\sqrt{\frac{1}{3}} \simeq 2$. On the other hand, the above sketched numbers for possible improvements of beam current and/or target density over the foreseeable time scale are very likely to compensate that loss, at least. Hence the sensitivities shown in the rest of the paper are believed to be about realistic for any type of a future polarized nucleon–nucleon scattering experiment running at HERA over 1 to 2 years. Any better estimate requires considerably intensified efforts to be invested along many different directions, like machine and target limitations, detector capabilities versus rate, spatial acceptance and costs etc.

The anticipated luminosity implies a full event rate of about $6 \cdot 10^5$ events/sec. This poses rather high requirements to both trigger and data acquisition although this rate will still be lower by more than one order of magnitude compared to *HERA-B*.

4 Kinematics

The basic motivation of this study is to explore the physics reach of measuring single and double spin asymmetries in fixed target nucleon–nucleon scattering at HERA. The kinematics of such measurements is basically constrained by the total energy $\sqrt{s} = 39.2$ GeV available for particle production. Hence the maximum transverse momentum of the produced particles is given by $p_T^{max} \simeq \sqrt{s}/2 = 19.6$ GeV/c.

Throughout the paper the usual set of kinematical variables characterizing a particle in the center of mass system will be utilized:

- $x_F = p_L/p_L^{max} \simeq 2 \cdot p_L/\sqrt{s}$ - Feynman variable
- $\eta = -\log\tan\frac{\Theta}{2}$ - pseudorapidity

All below cross section calculations for particular processes are either based on appropriately modified parametrizations of experimental data or utilizing the PYTHIA 5.7 and JETSET 7.4 Monte Carlo programs [46].

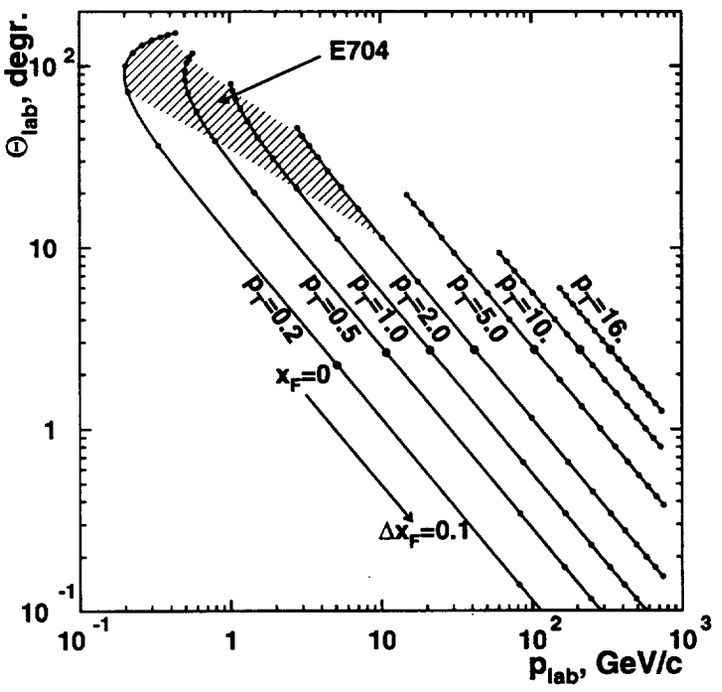

Figure 1: *Laboratory angle and momentum of inclusive pions as a function of p_T and x_F.*

It is instructive to illustrate the kinematics of single particle production in the plane of laboratory angle vs. laboratory momentum. In fig. 1 the interdependence between Θ_{lab} and p_{lab} for inclusive photon or pion production is shown as a function of x_F and p_T. The hatched area indicates the fragmentation region of the polarized nucleon where the E704 Collaboration has found significant non-zero values for the pion single spin asymmetry [23, 25]. For easier comparison this area is drawn in the backward hemisphere (target fragmentation region) since during phase I of HERA-$\vec{N}$ the *target* nucleon would carry the polarization, whereas in E704 the polarized *beam* was hitting an unpolarized target. It is obvious that in order to check the E704 results and to measure the hitherto unknown p_T dependence of single spin asymmetries at large enough x_F the spectrometer must be able to detect pions emitted under rather large laboratory angles ($\Theta_{lab} \gtrsim 10$ degrees) which simultaneously imply low momenta ($p_{lab} \lesssim 10$ *GeV/c*). As will be demonstrated in section 5.6, large angle coverage is also required if elastic nucleon–nucleon collisions should be investigated at the given beam energy.

On the other hand, the study of double spin asymmetries in direct photon and/or jet production during phase II of HERA-$\vec{N}$ would require to detect photons (and jets) also at rather small laboratory angles (a few tens of milliradians), as will be outlined in the following sections.
We note that the influence of the HERA-$\vec{N}$ spectrometer magnet to the polarization of the polarized proton beam, and possibly related restrictions to the minimal angle accesssible for particle detection, are beyond the scope of the present study.
Altogether it can be concluded that the HERA–$\vec{N}$ apparatus should have a wide-aperture spectrometer to ensure that a sufficiently broad spin physics program can be realized. A generic view of a possible apparatus is sketched in fig. 2 as top view assuming that the available length must not exceed about 10 m.

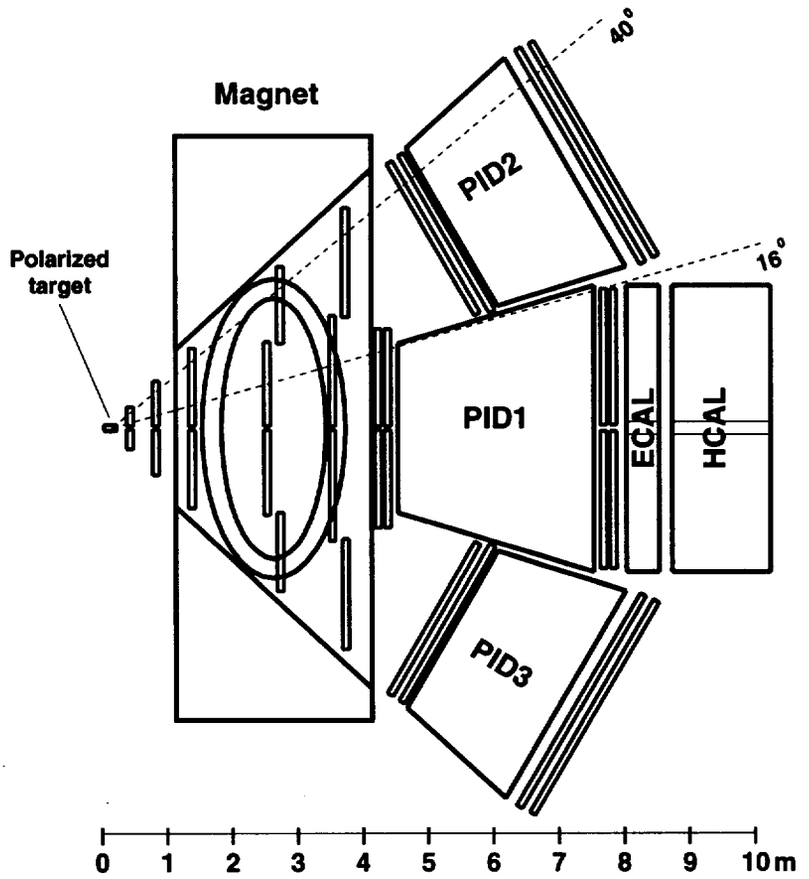

Figure 2: *Top view of a generic wide-aperture nucleon–nucleon polarization experiment at HERA.*

5 Physics Reach in Different Final States

5.1 Direct Photon Production

Single Spin Asymmetries.

Direct photon production $p + p^{\uparrow} \rightarrow \gamma + X$ proceeds without fragmentation, i.e. the photon carries directly the information from the hard scattering process. Hence this process measures a combination of initial $k_{\perp}$ effects and hard scattering twist–3 processes. The first and only results up to now were obtained by E704 [47] showing an asymmetry compatible with zero within large errors for $2.5 < p_T < 3.1$ GeV/c in the central region $|x_F| \lesssim 0.15$.

The experimental sensitivity of HERA-$\vec{N}$ was determined using PYTHIA 5.7 by simultaneous simulation of the two dominant hard subprocesses contributing to direct photon production,

- Gluon–Compton scattering $q + g \rightarrow \gamma + q$
- Quark–antiquark annihilation $q + \bar{q} \rightarrow \gamma + g$,

and of background photons that originate mainly from π^0 and η decays. The resulting sensitivity is shown in fig. 3 in dependence on x_F and p_T. An additional, more specific dependence on p_T is shown in fig. 13 on page 20.

Since we are eventually interested in measuring the p_T dependence of the underlying hard subprocesses separately, two operations have to take place simultaneously:

(i) Separation of the two hard scattering subprocesses by analysing them in different kinematical regions. The cross section ratio between them is expected to be larger than four for $p_T > 3$ GeV/c, i.e. for higher p_T the Gluon–Compton scattering dominates.

(ii) Separation of background photons which contribute their own asymmetry, caused by e.g. fragmentation effects. The best method is to select 'single' photons already in the trigger, hardware- or software-wise, by requiring no signal in a given cone around the photon.

With increasing p_T the rate of background photons decreases considerably faster than that of direct ones. This is illustrated in form of a dilution factor $D = N^{\gamma}_{non-direct}/N^{\gamma}_{direct}$, shown in fig. 4 in dependence on x_F and p_T. When multiplying in a given cell both the sensitivity and $\sqrt{1+D}$ the real sensitivity is readily obtained.

As can be seen from both figures, a good sensitivity (about 0.05) can be maintained up to $p_T \leq 8$ GeV/c. This is not anymore spoiled by neither the annihilation subprocess nor by background photons and should hence facilitate to detect a clear dependence of the direct photon single spin asymmetry on p_T.

We note that the admixture of background photons can be decreased already at lower p_T by a finer segmentation of the electromagnetic calorimeter. In this case a higher percentage of photons from π^0 decay can be identified and rejected, and the real dilution

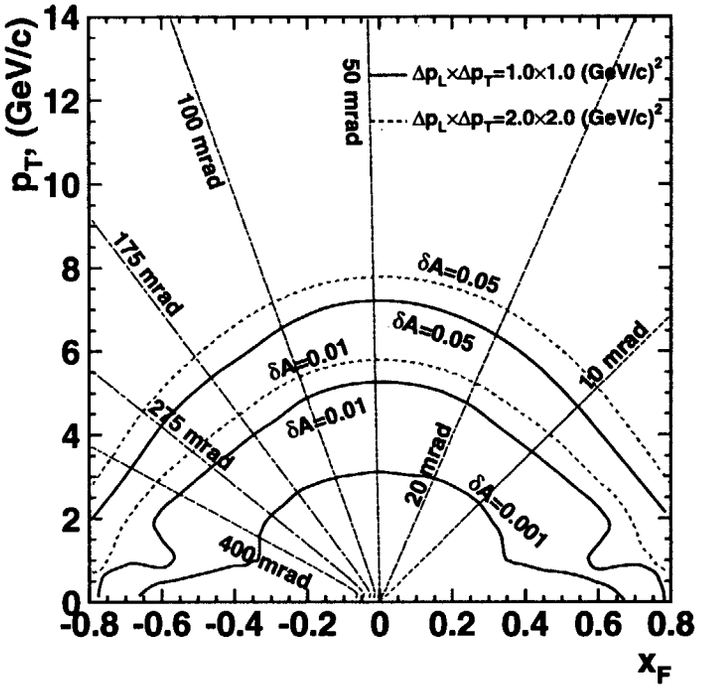

Figure 3: *Contours of the asymmetry sensitivity levels for photon production in the (p_T, x_F) plane. Lines of constant laboratory angles of photons are shown, in addition.*

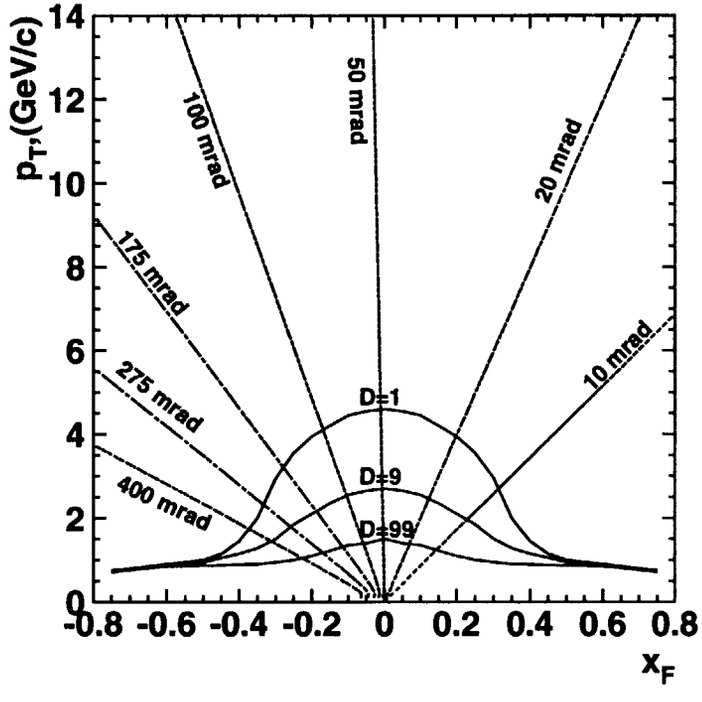

Figure 4: *Contours of the dilution factor for direct photon production in the p_T, x_F plane. Lines of constant laboratory angles of photons are shown.*

factor becomes smaller. The minimum angle Θ_{min} between photons from π^0 decay was calculated according to $\Theta_{min} \simeq 2 \cdot m_{\pi^0}/E_{\pi^0}$. The dependence of the corresponding minimum distance between photons from $\pi^0 \rightarrow 2\gamma$ decay after ten meters of flight is drawn in fig. 5 as a function of $p_T^{\pi^0}$ and the π^0 laboratory angle. It gives a first indication on the required minimum transverse granularity of the electromagnetic calorimeter.

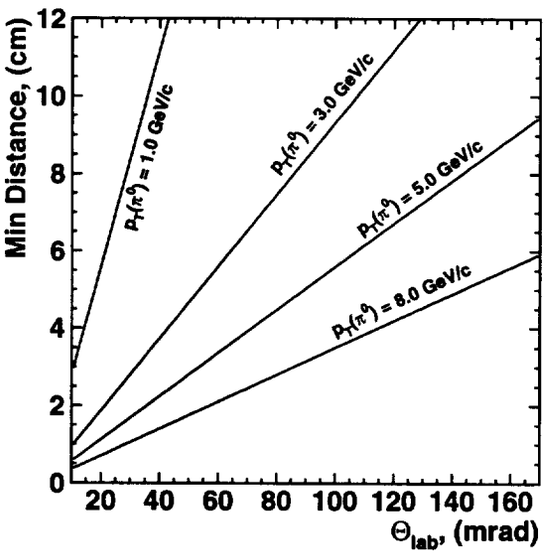

Figure 5: *Minimum distance between photons from* $\pi^0 \rightarrow 2\gamma$ *decay after ten meters flight as a function of the laboratory angle,* Θ_{lab}*, of* π^0 *for several values of the pion transverse momentum,* $p_T(\pi^0)$.

We note that in another approach one can compare data of both direct and background photons together, if the same is done in the corresponding simulation [48].

Double Spin Asymmetries.

The presently most accurate way to measure the polarized gluon distribution function in the nucleon is to study those processes which can be calculated in the framework of perturbative QCD, i.e. for which the involved production cross sections and subprocess asymmetries can be predicted. One of the cleanest ways to probe QCD is to measure direct photon production, because it is free from uncertainties due to fragmentation. Since the double spin asymmetry of the Gluon–Compton subprocess is large, it was already chosen as the premium candidate to measure the gluon polarization at RHIC [49].
In the following we investigate the corresponding capabilities of HERA–$\vec{N}$ when measuring direct photon production both inclusively and with additional detection of the away-side jet.

Inclusive high p_T photon production is described by a partonic formula proven within QCD factorization:

$$\Delta\sigma = \sum_f e_f^2 \int dx_1 dx_2 \Delta q(x_1) \Delta G(x_2) \Delta\hat{\sigma}(x_1, x_2) + (x_1 \leftrightarrow x_2) \qquad (7)$$

Here the integration of the difference of the partonic Compton cross sections with definite helicities is performed in a region defined by the following system:

$$0 \leq x_1, x_2 \leq 1, \quad 1 - \frac{\sqrt{x_T^2 + x_F^2} + x_F}{2x_1} - \frac{\sqrt{x_T^2 + x_F^2} - x_F}{2x_2} = 0 \tag{8}$$

The symmetrization accounts for the possibility to get either quark or gluon from both beam and target proton. The asymmetry is obtained by dividing formula (7) by the analogous expression for the spin averaged cross section:

$$\sigma = \sum_f e_f^2 \int dx_1 dx_2 q(x_1) G(x_2) \hat{\sigma}(x_1, x_2) + (x_1 \leftrightarrow x_2) \tag{9}$$

The additional quark–antiquark annihilation subprocess is assumed to be suppressed because of the lower density of antiquarks compared to gluons.
The main contribution to the integrals is coming from the region $x_1 \sim x_2$ because of the rapid decrease of the parton distribution when $x \to 1$. However, the Monte-Carlo simulation shows that this region appears to be rather wide. It therefore needs a more detailed study to determine how well in this situation the polarized gluon distribution can be obtained by an iterative fitting procedure to the experimental data.

To illustrate that there is reasonable hope to extract significant information on ΔG(x) the asymmetry for inclusive photon production is shown in fig. 6 vs. x_F in several different p_T bins. It was calculated with SPHINX [50] utilizing both Gluon–Compton and $q\bar{q}$ in the known proportion. Set A of Gehrmann-Stirling parametrization [51] for $\Delta G(x)$ was used as input. As can be seen from the projected statistical errors for 240 pb^{-1}, drawn in fig. 6 as well, there is sufficient accuracy available up to $p_T \leq 8$ GeV/c.

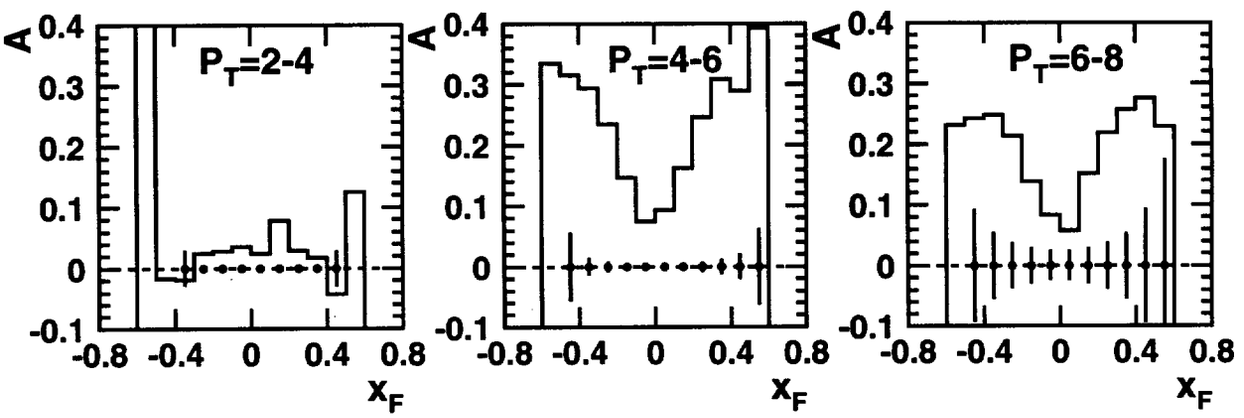

Figure 6: *Double-spin asymmetry as a function of x_F in different intervals of p_T for direct photon production as predicted by SPHINX MC program [50] using set A of Gehrmann-Stirling distributions [51] for polarized nucleon. The projected sensitivity of HERA-$\vec{N}$ is shown.*

Photon plus jet production allows for a direct determination of the polarized gluon distribution at several points, since the measurement of the away-side jet balancing the photon transverse momentum leads to an additional constraint:

$$x_1 - x_2 = x_F^{tot} \equiv x_F^{\gamma} + x_F^{jet} \tag{10}$$

The integrations in Eq.'s (7) and (9) are then removed and the cross sections are given by the integrated functions:

$$\Delta\sigma = \sum_f e_f^2 \Delta q(x_1)\Delta G(x_2)\Delta\hat{\sigma}(x_1,x_2) + (x_1 \leftrightarrow x_2), \tag{11}$$

$$\sigma = \sum_f e_f^2 q(x_1)G(x_2)\hat{\sigma}(x_1,x_2) + (x_1 \leftrightarrow x_2), \tag{12}$$

Here x_1, x_2 are the solutions of the system (8), which are especially simple if $x_F^{tot} = 0$, i.e. if the x_F values of photon and jet are equal in magnitude and opposite in sign:

$$x_1 = x_2 = \sqrt{x_T^2 + x_F^2} \tag{13}$$

As a result, the symmetrizing term in (7) and (9) appears to be equal to the original one and another simplification appears:

$$\Delta\sigma = \sum_f e_f^2 \Delta q(x_g)\Delta G(x_g)\Delta\hat{\sigma}(x_g) \sim g_1(x_g)\Delta G(x_g)\Delta\hat{\sigma}(x_g) \tag{14}$$

$$\sigma = \sum_f e_f^2 q(x_g)G(x_g)\hat{\sigma}(x_g) \sim F_1(x_g)G(x_g)\hat{\sigma}(x_g), \tag{15}$$

Here the quark and gluon momentum fractions are the same:

$$x_q = x_g = \sqrt{x_T^2 + x_F^2} \tag{16}$$

In Equ.'s (14) and (15) we had already chosen the subscript g to underline that it is the gluon distribution which is of primary interest. It is important to note that therefore data points located in a corridor around lines of constant x_g in the (x_F, x_T) plot contribute to the same bin in the polarized gluon distribution. In other words, when collecting all experimental data on the double spin asymmetry in appropriate circular bins of the (x_F, x_T) plane the obtained asymmetry in this bin directly corresponds to the x_g value given by (16).

Since the combination of quark distributions appearing in the cross sections is just the same as that entering the definition of the structure functions F_1 and g_1, it is now straightforward to define the double spin asymmetry of direct photon plus jet production:

$$A_{LL} = A_{DIS} \cdot \hat{a}_{LL} \cdot \frac{\Delta G(x_g)}{G(x_g)} \tag{17}$$

Here the partonic level asymmetry $\hat{a}_{LL}$ [57] is easily reduced to the form

$$\hat{a}_{LL} = \frac{3 - 2\bar{x}_F^2 - \bar{x}_F^4}{5 + 10\bar{x}_F^2 + \bar{x}_F^4}, \tag{18}$$

where $\bar{x}_F = x_F/x_g$. This function is monotonically decreasing when $\bar{x}_F$ is growing, while the partonic matrix element is increasing like $\bar{x}_T^4 = (1 - \bar{x}_F^2)^2$.
At this point we have to consider the influence of the acceptance. Adopting the experience gained in the preliminary study of jet reconstruction (cf. section 5.3) and taking into account that photon and jet have always to obey $x_F^{tot} \simeq 0$, we choose the region of $-0.5 \leq \eta_{CMS} \leq 1.0$ for the photon and, correspondingly, $-1.0 \leq \eta_{CMS} \leq 0.5$ for the jet. The acceptance of the detector then yields $\bar{x}_F \sim 0.78$ for forward photons and backward jets, and $\bar{x}_F \sim 0.51$ for backward photons and forward jets, respectively.

The absolute statistical error of $\Delta G(x_g)/G(x_g)$ is readily obtained as

$$\delta[\frac{\Delta G(x_g)}{G(x_g)}] = \frac{\delta A_{LL}}{A_{DIS} \cdot \hat{a}_{LL}}. \tag{19}$$

where A_{DIS} and $\hat{a}_{LL}$ are to be taken at the appropriate values of $\bar{x}_F$ and x_g, respectively.

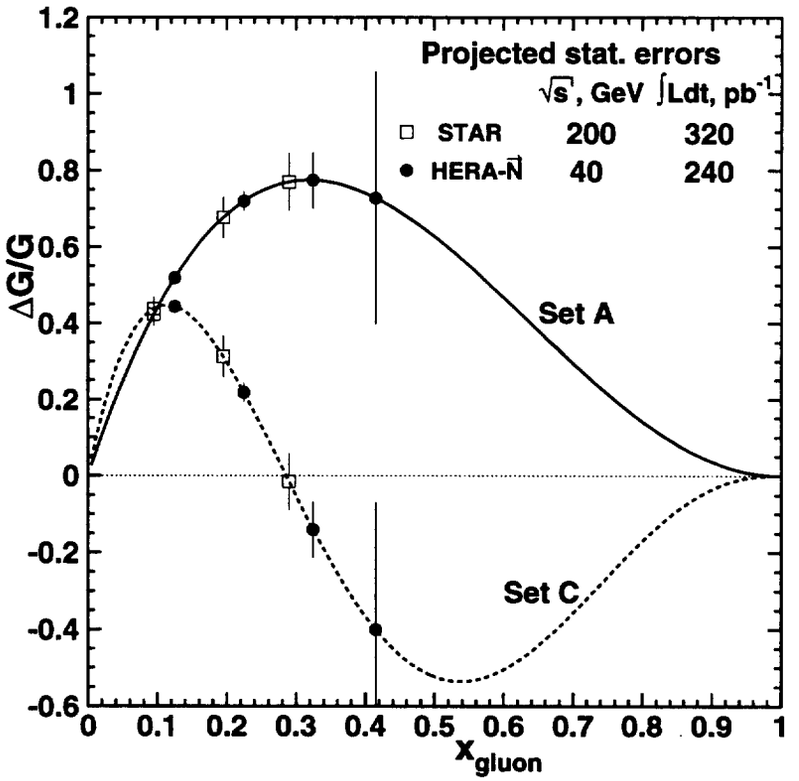

Figure 7: *Typical predictions for the polarized gluon distribution confronted with the projected statistical errors expected for HERA-$\vec{N}$ and RHIC experiments.*

In fig. 7 we reproduce two typical predictions for the polarized gluon distribution (Gehrmann and Stirling [51], set A and C) in conjunction with the projected HERA-$\vec{N}$ statistical errors obtained after the data has been analyzed in the above described way. The errors demonstrate clearly that in the region $0.1 \leq x_g \leq 0.4$ a significant result can be expected. This statement will very probably remain valid if once the systematic errors will have been estimated. Note that in this first approximation the jet and photon reconstruction efficiences were not included, yet. From preliminary jet studies (cf. section 5.3) it can be anticipated that a serious deterioration might occur for lower p_T-values only, i.e. for the left-most point in fig. 7.
For comparison, we show the corresponding projected statistical errors for *STAR* running at 200 GeV c.m. energy [52]. As can be seen, the measurement of $\Delta G(x_g)/G(x_g)$ in doubly polarized nucleon-nucleon collisions at HERA can be presumably performed with an accuracy being about competitive to that predicted for RHIC. A word of caution has to be added: the projected RHIC errors available today base upon much more detailed studies than those shown here for HERA.

5.2 Pion Production

Significant non-zero single spin asymmetries were measured a few years ago by the E704 Collaboration in inclusive pion production $p^{\uparrow} + p \rightarrow \pi^{0\pm} + X$ using a transversely polarized beam at 200 GeV [23, 25] (see fig. 8). For any kind of pions the asymmetry A_N was found to exhibit a considerable rise above $x_F > 0.3$, i.e. in the fragmentation region of the polarized nucleon. It is positive for both π^+ and π^0 mesons, while it has the opposite sign for π^- mesons. The charged pion data taken at $0.2 < p_T < 2$ GeV were split into two samples at $p_T = 0.7$ GeV/c; the observed rise is stronger for the high p_T sample.

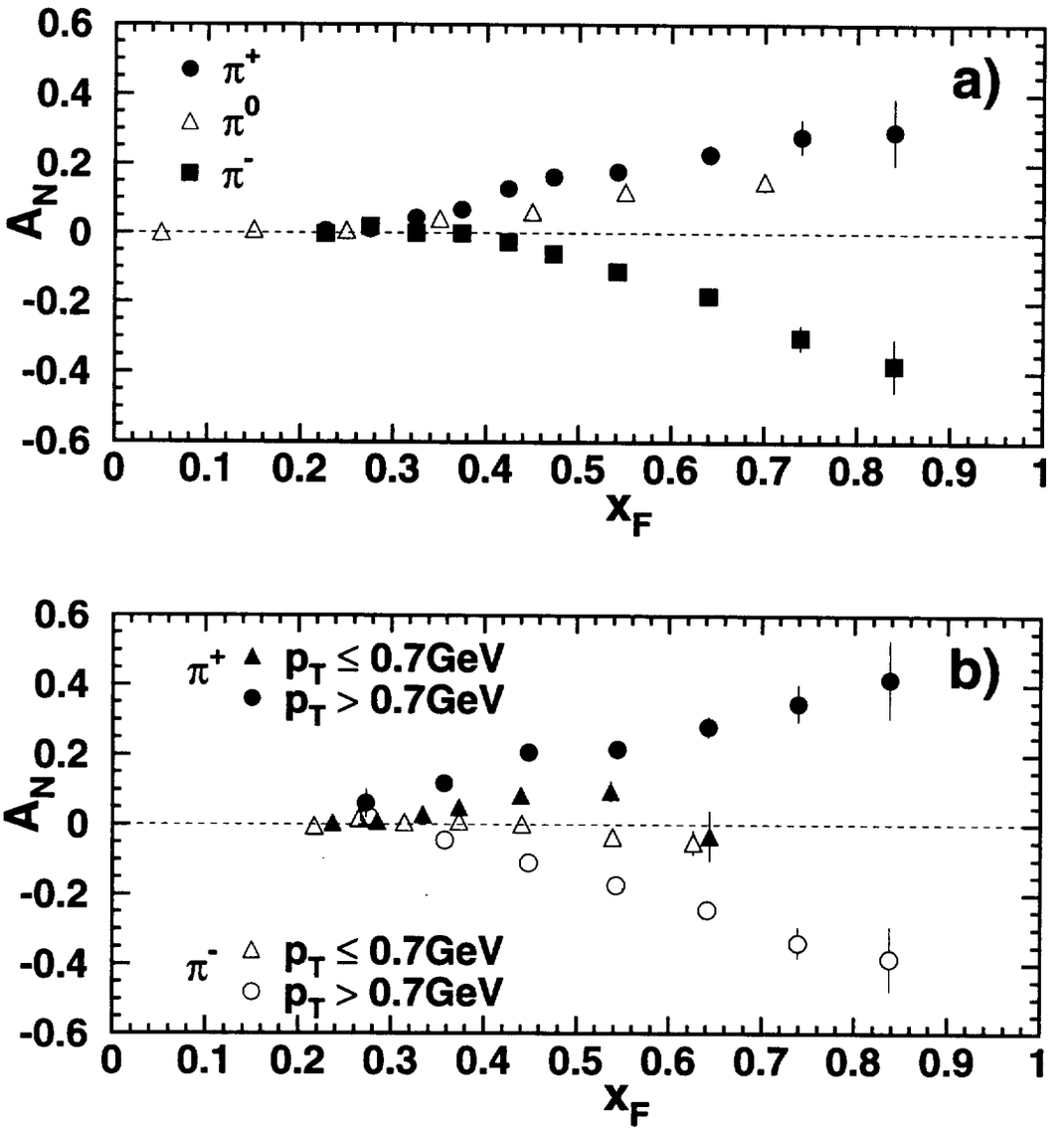

Figure 8: *Single spin asymmetry in inclusive pion production* $p^{\uparrow} + p \rightarrow \pi^{0\pm} + X$ *measured by the E704 Collaboration [23, 25] as a function of* x_F. *a) data averaged over the whole* p_T *region; b) data split into two subregions of* p_T.

The **inclusive π^+ production** differential cross section in the HERA-$\vec{N}$ kinematical region is required to estimate the sensitivity δA_N on the left-right asymmetry A_N. Data on inclusive π^0 production at beam energies between 100 and 300 GeV were parametrized as [53]

$$\frac{d^2\sigma}{dp_T dx_F} = A\frac{\pi p_T\sqrt{s}}{E}\frac{(1-x_d)^F}{(p_T^2+m^2)^N}, \tag{20}$$

where

$$x_d = (x_T^2 + (x_F - x_0)^2)^{\frac{1}{2}}.$$

This parametrization was normalised to take into account the difference in the production cross sections of π^+ and π^0. In fig. 9 the prediction of this parametrization is compared to experimental data taken at $\sqrt{s} = 44 \div 45$ GeV [54, 55] which is close to HERA-$\vec{N}$ energies. Two other parametrizations [55, 56] are shown for comparison. Good agreement between the parametrization [53] and the available experimental data is found over a wide range of p_T values.

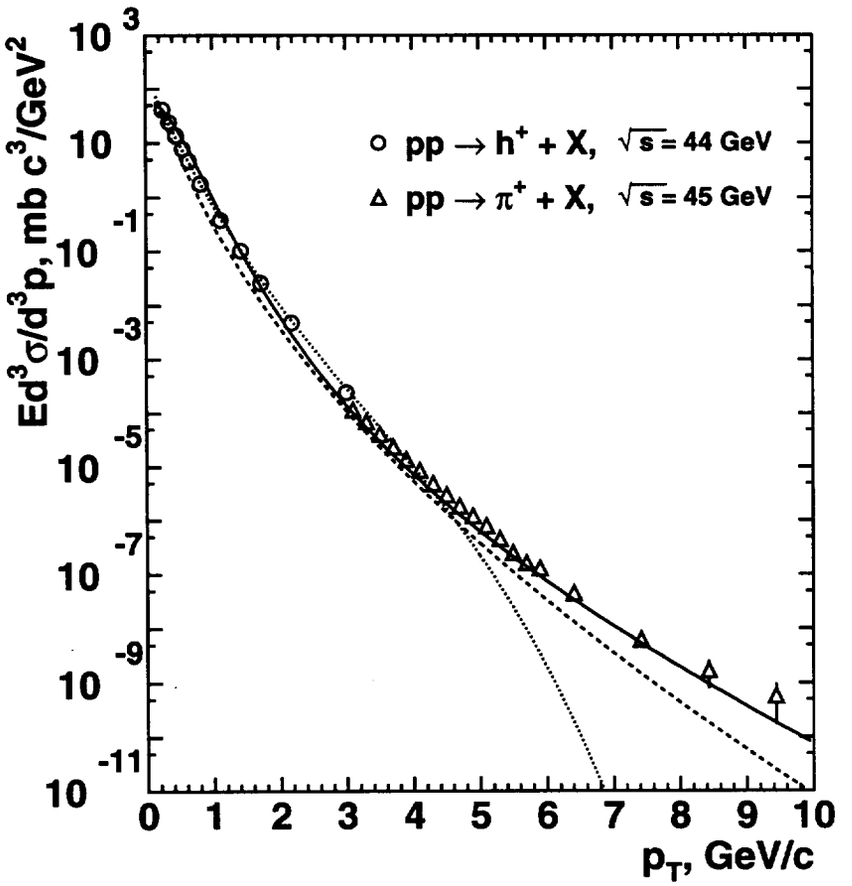

Figure 9: *Invariant cross section as a function of p_T at $< |y| >= 0.75$ for positive particles (circles) at $\sqrt{s} = 44$ GeV [55] and positive pions (triangles) at $\sqrt{s} = 45$ GeV [59]. Several kinds of parametrizations are shown: dotted line - Ref. [55], dashed line - Ref. [56]. The solid line corresponds to the parametrization (20) in sect. 5.2, as used to estimate the π^+ production cross section at HERA-$\vec{N}$ energies.*

In fig. 10 contours are shown to characterize several sensitivity levels ($\delta A_N = 0.001$, 0.01 and 0.05) for an asymmetry measurements in the reaction $p + p^{\uparrow} \rightarrow \pi^+ + X$ under the above explained HERA-$\vec{N}$ conditions. Note that in the large p_T region the contours calculated with big $\Delta p_L \times \Delta p_T$ bins are appropriate, since usually a larger bin size is chosen where the statistics starts to decrease.
We can conclude that the accessible p_T values are significantly larger than those E704 had. The combined p_T dependence of all involved higher-twist effects can be measured with good accuracy ($\delta A_N \leq 0.05$) up to transverse momenta of about 10 GeV/c in the central region $|x_F| < 0.2$ and up to 6 GeV/c in the target fragmentation region.

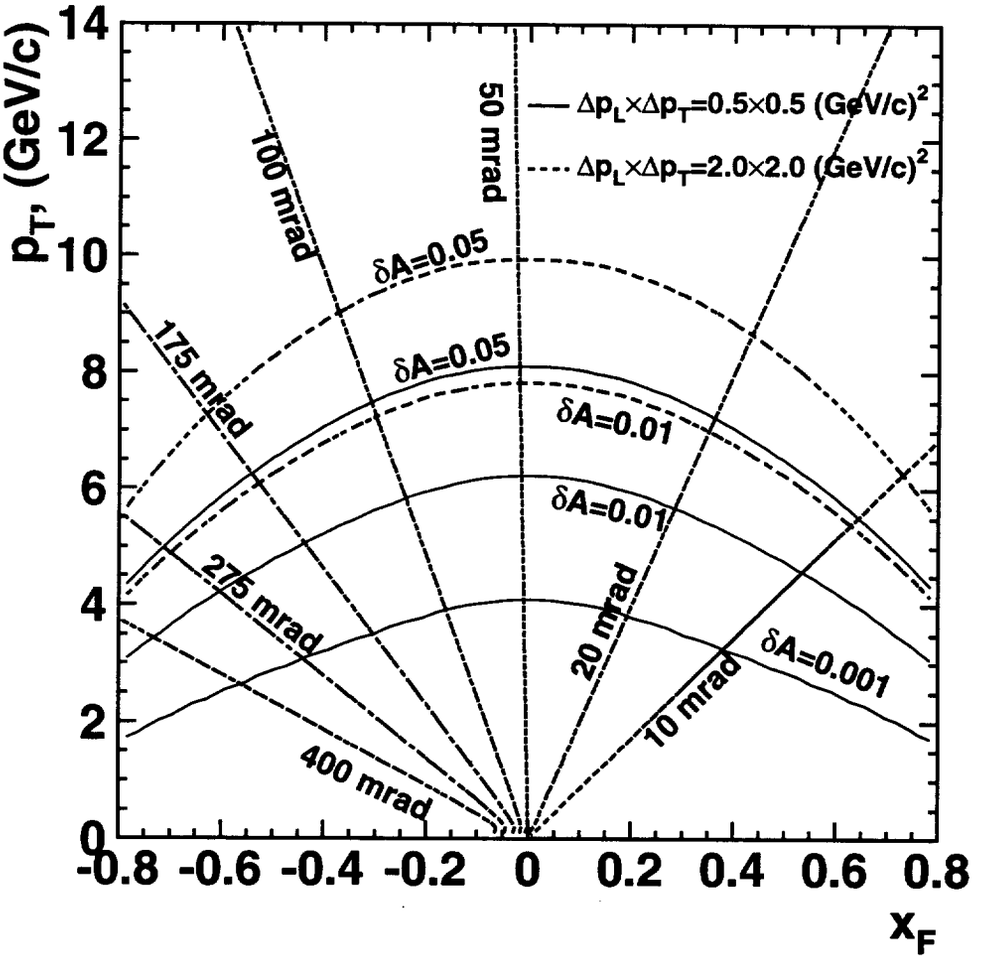

Figure 10: *Contours of the asymmetry sensitivity levels for π^+ production in the (p_T, x_F) plane. Lines of constant laboratory angles of the pion are shown.*

To make sure that the genuine p_T dependence of the single spin asymmetry is not spoiled by other implicit dependencies we write it in its most general form as predicted by kinematics and dimensional analysis:

$$A_N = \frac{M}{p_T} f(x_F, x_T) \tag{21}$$

In a good approximation the energy dependence can be neglected. This allows for a simplification:

$$A_N = \frac{M}{p_T} f(\tilde{x}_F)\,, \tag{22}$$

where $\tilde{x}_F = x_F/x_T$. This behaviour can be clearly checked if the data is binned in an appropriate way, i.e. along angular sectors having the same $\tilde{x}_F$ value. As indicated in fig. 11 each angular sector, when considering a certain region of high, i.e. target fragmentation like x_F values (say, -0.4 to -0.8), covers a rather small range in p_T, only. Each of these sectors being characterized by a certain average $\tilde{x}_F$ then delivers its own p_T dependence which is scaled among each other by the difference in the function $f(\tilde{x}_F)$. Taken all $\tilde{x}_F$ bins together, a clear picture is supposed to emerge on the overall p_T dependence of higher twist effects. The sensitivity within each sector vs. p_T is displayed in fig. 12 for pion production and in fig. 13 for photon production. As can be seen, there is good sensitivity ($\delta A_N \leq 0.05$) up to $p_T \simeq 10$ GeV for pions and up to $p_T \simeq 8$ GeV for photons. In π^- and π^0 production the estimated sensitivities are very close to the one in π^+ production. This can be seen from the cross section ratio of $\sigma(\pi^-)/\sigma(\pi^+)$ measured at high p_T values [58, 59], and from the approximate relation $\sigma(\pi^0) = (\sigma(\pi^+) + \sigma(\pi^-))/2$.

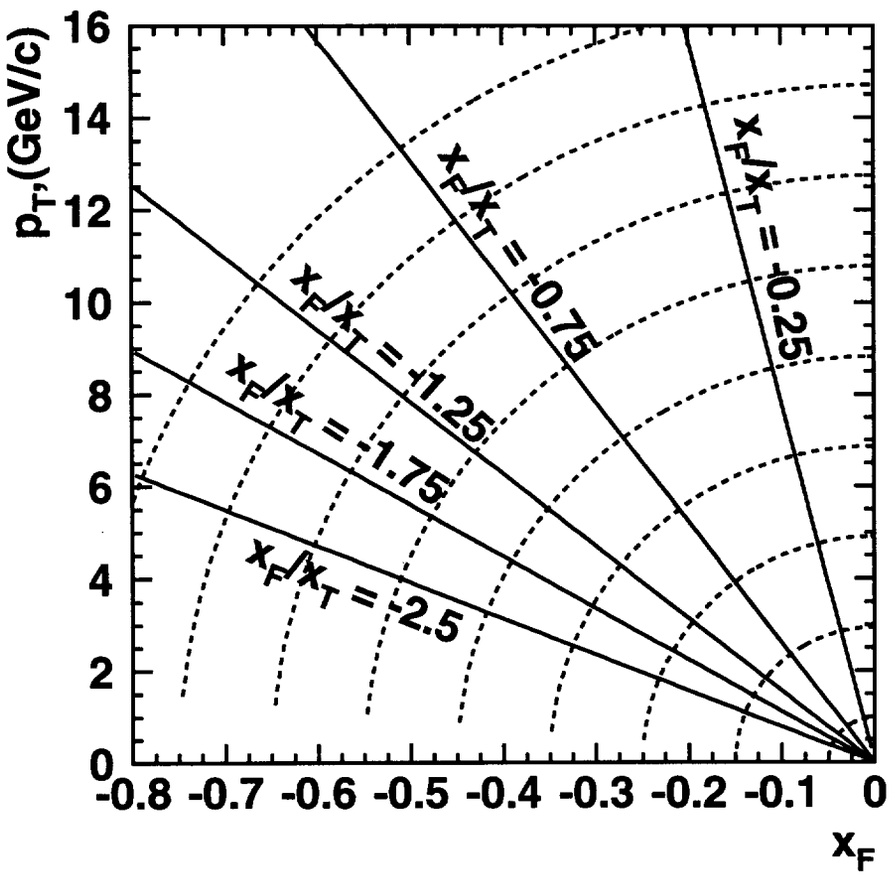

Figure 11: *Sectors of equal $\tilde{x}_F = x_F/x_T$ to collect statistics.*

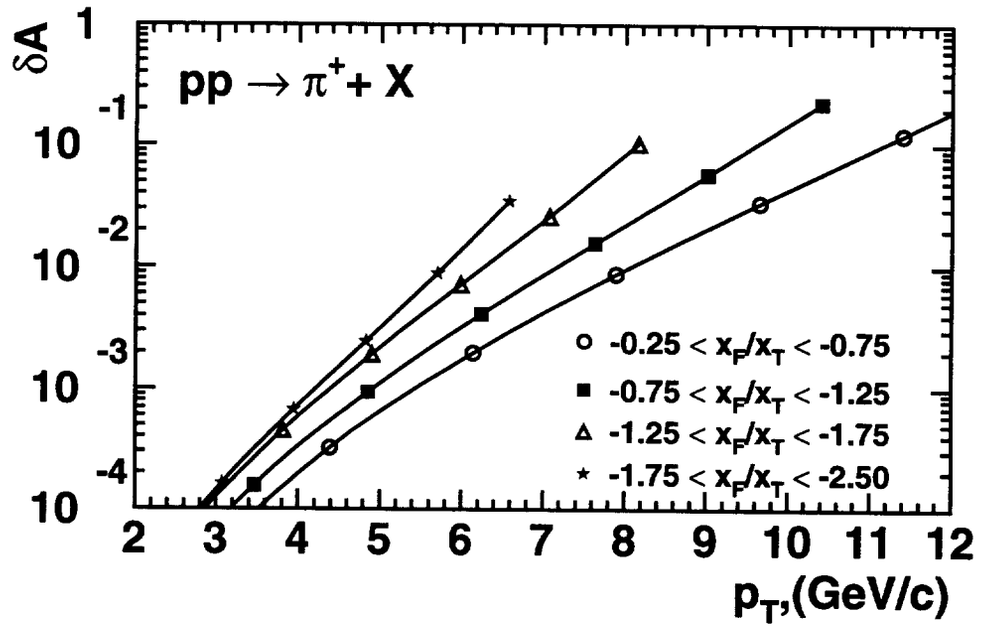

Figure 12: *Projected statistical accuracy vs. p_T in the different sectors of fig. (11) for pion production.*

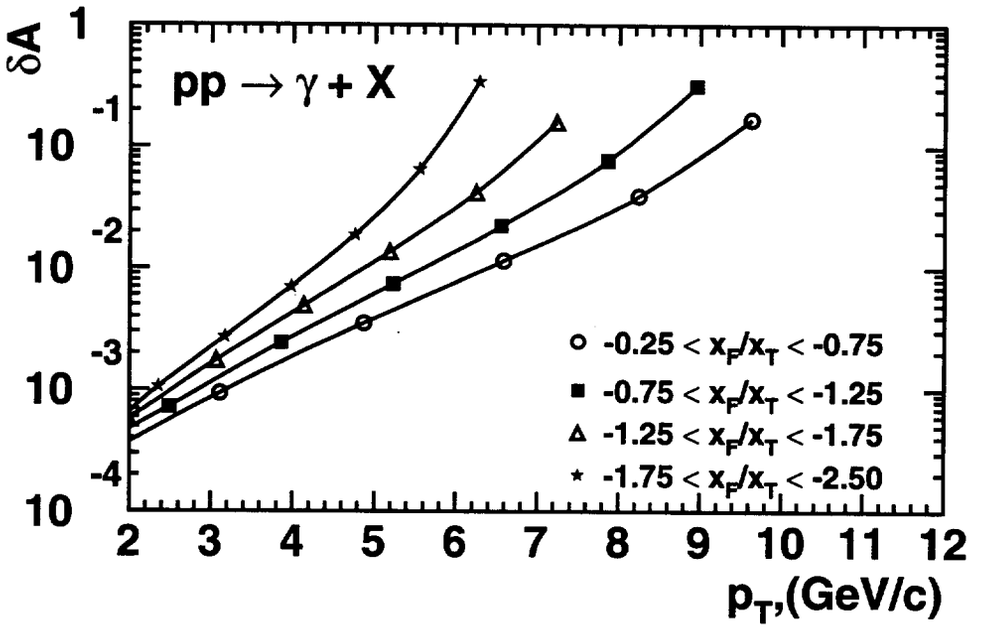

Figure 13: *Projected statistical accuracy vs. p_T in the different sectors of fig. (11) for photon production.*

5.3 Jet Production

The measurement of spin asymmetries in inclusive jet production $p + p^{\uparrow} \rightarrow jet + X$ benefits from the highest counting rate when comparing to other inclusive final states. In addition, it is almost free of fragmentation problems if an efficient jet finding algorithm can be applied.

Jet production was simulated with PYTHIA 5.7 taking into account all possible $2 \rightarrow 2$ subprocesses. The resulting sensitivity to an asymmetry measurement under HERA-$\vec{N}$ conditions is displayed in the (x_F, p_T) plane in fig. 14; again the big bins should be considered when assessing the sensitivity at larger p_T values. In the central region $|x_F| \leq 0.2$ the large jet production cross section allows to measure asymmetries with good accuracy ($\delta A \leq 0.05$) up to $p_T = 14\ GeV/c$ and even in the target fragmentation region, say $-0.8 < x_F < -0.4$, any p_T dependence can be detected up to transverse momenta of about 8 GeV/c.

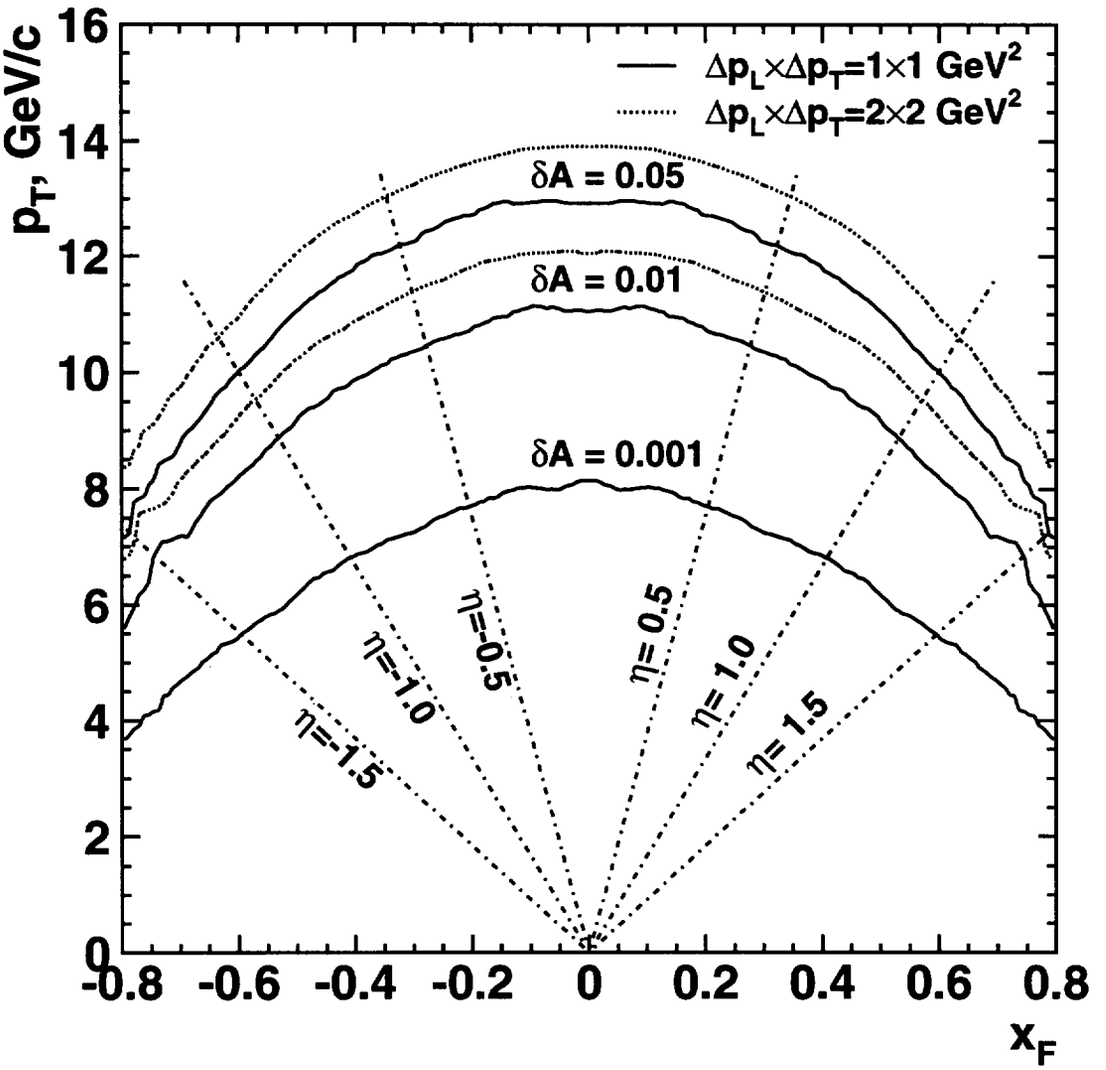

Figure 14: *Contours of the asymmetry sensitivity levels for jet production in the (p_T, x_F) plane. Lines of constant pseudorapidity in the CMS of the event are shown.*

The reconstruction of jets in a fixed target experiment is not an easy task and must be investigated carefully. Here we report on the results of a preliminary study. We applied the UA1 cone algorithm, utilized usually in hadron collider experiments, which exploits the calorimetric information on the transverse energy deposited by the produced particles. The algorithm starts with a search for the maximum local transverse energy in the $(\eta - \phi)$ plane, which should exceed some predefined threshold value E_T^i. Then the sum of the transverse energies in a cone with radius $R = \sqrt{(\Delta\eta)^2 + (\delta\phi)^2} \leq R_0$ around this maximum is calculated and assigned to be the jet energy if being larger than a threshold E_T^{sum}.

The most important specific feature exhibited by jets when produced in a fixed target environment is that during the transition from CMS to the laboratory system the Lorentz boost strongly modifies the size of the jet cone in space, $\eta_{lab} = \eta_{CMS} + \Delta\eta_{CMS}$, where $\Delta\eta_{CMS} \simeq 3.73$ at HERA-$\vec{N}$ energies. As a result jets emitted forward in CMS are projected to (very) small laboratory angles, whereas those emitted backwards in CMS are widened up considerably.
Future studies need to take advantage of these specific features. Possibly global event variables like planarity may play a useful role in jet reconstruction.

The efficiency of jet registration under HERA-$\vec{N}$ conditions was investigated at the particle level applying the cone algorithm with $R_0 = 1.2$ to Monte-Carlo events. A calorimeter, consisting along the particle's path of an electromagnetic one followed by the hadronic part, was located at 10 m distance from the target. A central hole with radius R_h is required for the beam pipe. A transverse cell granularity of 5×5 cm^2 is assumed. A resolution of $\Delta E/E = 10\%/\sqrt{E} \oplus 1\%$ is assigned to the electromagnetic part, wheras for the resolution of the hadronic one $\Delta E/E = 70\%/\sqrt{E} \oplus 2\%$ is taken. Charged particle trajectories were subject to a magnetic field providing a transverse momentum kick of 0.45 GeV/c. Two different versions were investigated for both the calorimeter transverse dimensions (6×6 m^2 and 4×4 m^2) and the inner hole ($R_h = 10$ and 20 cm).
Two typical examples for jet events as seen by the calorimeter are displayed in fig. 15 for jets with $p_T \simeq 5$ GeV/c [(a), (b)] and with $p_T \simeq 9$ GeV/c [(c), (d)]. The left side of the figure [(a), (c)] shows the distribution of the transverse energy across the calorimeter wall for *all* particles belonging to the particular event, while the right side [(b), (d)] shows the transverse energy deposited by particles originating from the *jets, only.* At the present level of investigation it can be concluded that at large enough p_T values the task of jet reconstruction seems not at all hopeless.

A more quantitative confirmation of this statement can be seen in fig. 16, where preliminary results on the jet reconstruction efficiency as a function of η_{jet} are presented for several consecutive ranges of jet transverse momenta. The different line types drawn denote the above explained different calorimeter dimensions (see figure captions). As can be seen, the transverse size of the calorimeter plays a certain role in the CMS backward hemisphere, while the diameter of the central hole is a very critical value for the registration of jets emitted into the CMS forward hemisphere. Nevertheless, the efficiency is found to be surprisingly large in the rapidity region $-1.5 \lesssim \eta_{CMS} \lesssim 0. \div 0.5$.

We must note, however, that the above results were obtained by a rather simplified method. To understand the real feasibility of jet reconstruction in HERA-$\vec{N}$ a much more detailed study will have to be performed. Another important question not studied yet is a possible contamination of "false jet" events which may be simulated by non-jet events.

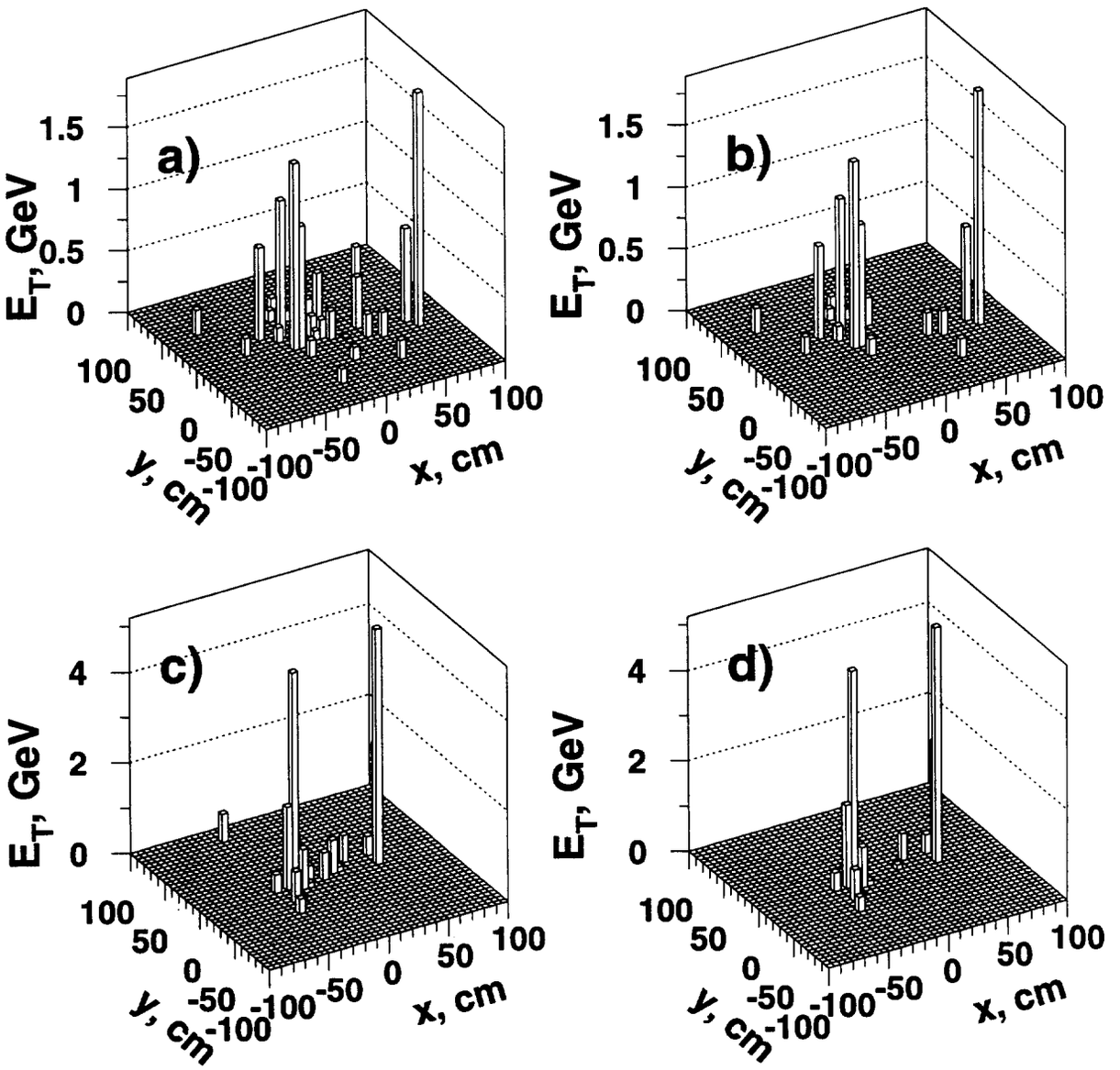

Figure 15: *Transverse energy distributions for two-jet events across the calorimeter wall.*

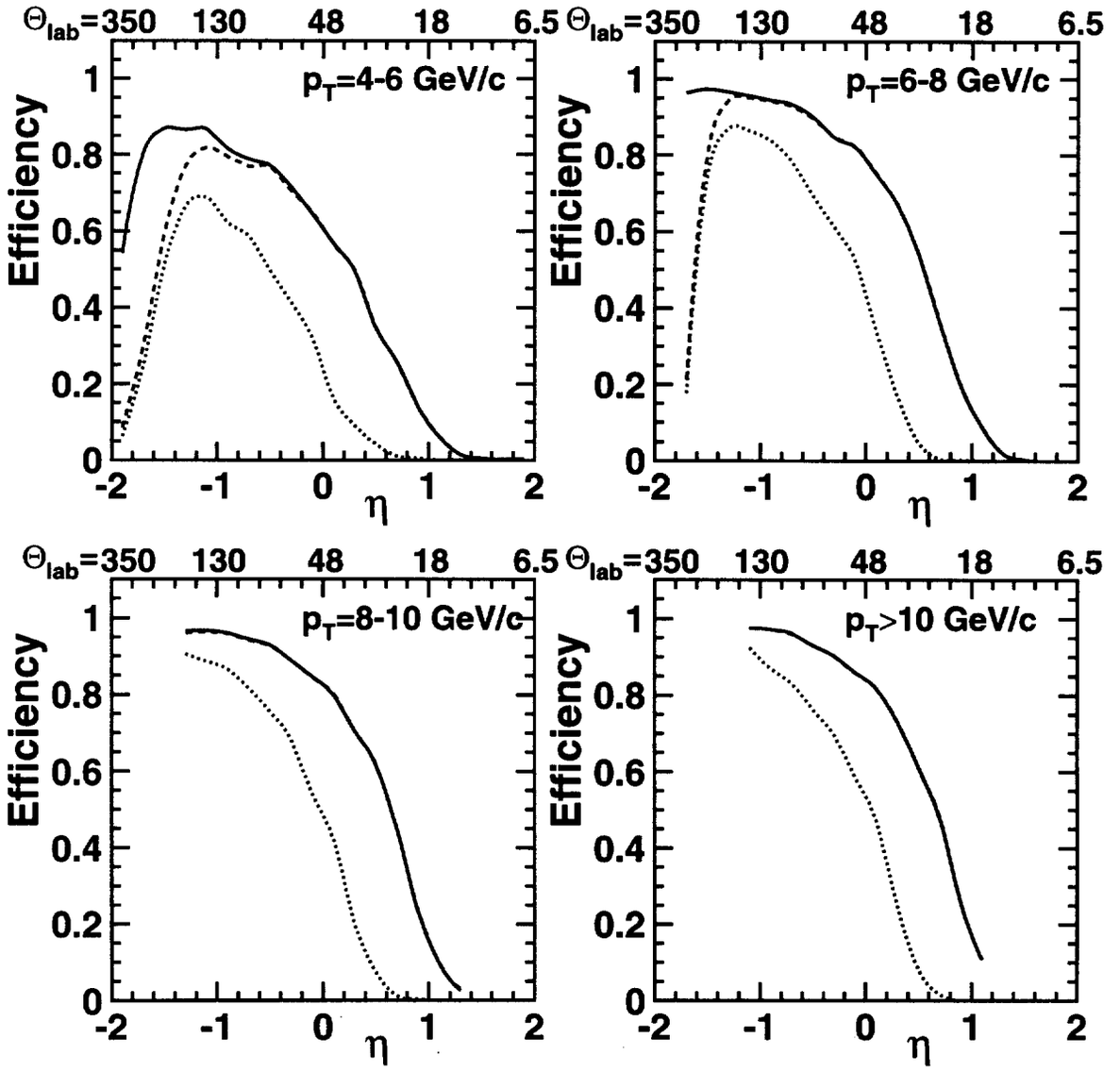

Figure 16: *Jets registration efficiency as a function of their pseudorapidity, η, in the CMS for several regions of jet transverse momenta p_T. At the top scale the laboratory angles (mrad) corresponding to the CMS pseudorapidity are shown. Several versions of the calorimeter geometry are considered:*
i) solid line - transverse dimension of $6 \times 6m^2$, *central hole radius of* 10 *cm;*
ii) dashed line - transverse dimension of $6 \times 6m^2$, *central hole radius of* 20 *cm;*
iii) dotted line - transverse dimension of $4 \times 4m^2$, *central hole radius of* 20 *cm.*

5.4 J/ψ Production

Compared to direct photon production the production of quarkonium states below the open charm threshold is a similarly clean tool to measure the polarized gluon distribution. Hence many of the statements made in section 5.1 apply here, as well, and the principle of analysis is very similar. Because of the relatively large quark mass the $c\bar{c}$ production cross section and the expected asymmetry are supposed to be calculable perturbatively.

The production of bound states of heavy quarks has been theoretically studied in terms of the colour singlet mechanism [62]. In this approach the dominant contribution is expected to come from quark-antiquark or gluon-gluon fusion, leading to the formation of the heavy quark pair in a colour singlet state with the correct spin, parity, and charge conjugation assignments projected out. Although the colour singlet mechanism describes successfully the J/ψ production cross section shapes over p_T and x_F at ISR and Fermilab fixed target energies ($\sqrt{s} \simeq 30 \div 60$ GeV) [63], it completely fails to explain the integrated cross section. Hence a K-factor of about 7 needs to be introduced to restore agreement in magnitude.

Recent improvements in the theory of quarkonium production have been stimulated by the anomalously large cross section for J/ψ production at large p_T as measured recently in the CDF experiment at the Tevatron [64]. The CDF data has been explained by taking into account additionally the colour octet mechanism of heavy quarkonium production [65]. However, it is not obvious at all that the colour octet mechanism is already at work for the relatively low energies $\sqrt{s}$ of about $30 \div 60$ GeV, because the contradiction between the experimental data and the colour singlet predictions appears only in the cross section magnitude and not in the differential cross section shapes. In addition, predictions from the color octet mechanism appear at variance with recent experimental data obtained at HERA [66] indicating that its phenomenological importance is smaller than expected from theoretical considerations and suggested by the Tevatron fits [67].

The **single spin asymmetry** in inclusive J/ψ production was calculated in the framework of the colour singlet model [68]. The results of our calculations at HERA energies are presented in fig. 17. For a first estimate of the expected asymmetry we used the polarized gluon distribution by Gehrmann and Stirling [51]. As one can see, the asymmetry effect is less than 0.01 in the region $|x_F| < 0.6$ and when taking into account the dilution caused by the large K-factor it will become practically unobservable.

The **double spin asymmetry** was calculated [69] in the framework of the colour singlet model, as well. As can be seen from fig. 18, the resulting asymmetry at $p_T = 2.5$ GeV is rather large (about 0.2) in the central region of x_F for the hard Gehrmann-Stirling distribution, but very small for the soft one.
The clarification of possible contributions from other sources leading to J/ψ's in the final state requires a separate study. The $\chi_2(3555)$ double spin asymmetry being large and *negative* [70] should lead to dramatic changes in the asymmetry at low p_T, where this mechanism is essential. It would then be especially important to discriminate between direct J/ψ's and those originating from $\chi_2 \rightarrow$J/$\psi + \gamma$ decays. Experimentally this seems well feasible since the spectrometer has to be anyway optimized for photon detection.

The direct mechanism becomes dominant at $p_T = 2.5$ GeV. The asymmetry due to fragmentation is actually that of Born gluon-gluon scattering [57], but the relative weight of this contribution at different p_T has still to be studied.

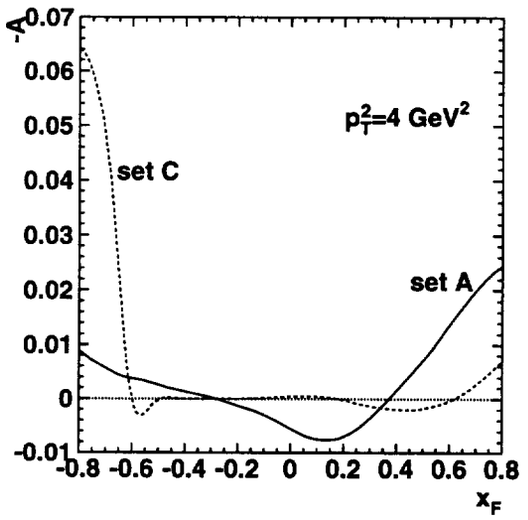

Figure 17: *Single-spin asymmetry in inclusive $J/\psi \rightarrow e^+e^-$ production. Solid curve - hard Gehrmann-Stirling distribution (set A), dashed curve - soft distribution (set C).*

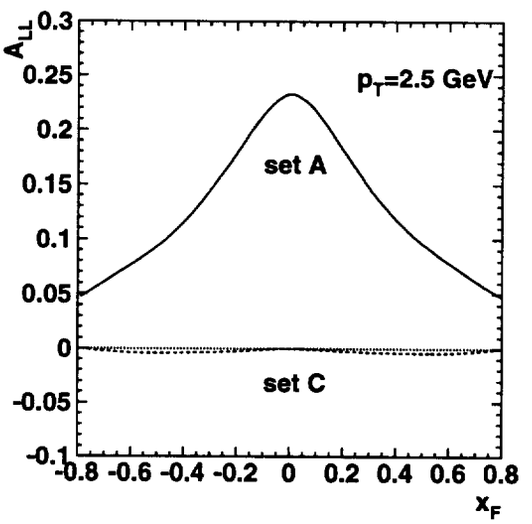

Figure 18: *Double-spin asymmetry in inclusive $J/\psi \rightarrow e^+e^-$. production. Solid curve - hard Gehrmann-Stirling distribution (set A), dashed curve - soft distribution (set C).*

We calculated the expected statistical sensitivity for the spin asymmetry in J/ψ production. The J/ψ production processes and their decay into e^+e^--pairs were simulated with PYTHIA 5.7 taking into account all possible $2 \rightarrow 2$ subprocesses. The total cross section was normalized to the Fermilab data on 800 GeV/c proton–gold collisions [63]. We cut the J/ψ transverse momentum at $p_T > 1$ GeV since at smaller p_T the expected asymmetry is negligible. The detection of the lepton pair was assumed to be done with an electromagnetic calorimeter situated at 10 m distance from the target with transverse dimensions of 6×6 m^2 and an inner hole with 10 cm radius. As can be seen from fig. 19, there is good sensitivity in the central region up to $p_T \leq 4$ GeV.

It is important to note that if the colour singlet mechanism could be isolated by detecting the away-side jet this would allow to probe the polarized gluon distribution at several x_g values, similar to the case of photon plus jet (cf. section 5.1). When comparing the sensitivities shown in fig. 3 (inclusive photon production) and fig. 19 the reach in p_T is found about twice as large for photons compared to J/ψ's. The apparently rather different behaviour of the hard scattering asymmetry, seen when comparing fig.'s 6 and 18, indicates that nevertheless both final states might yield complementary information on the polarized gluon distribution.

Hence from future studies it might turn out that the double spin asymmetry in J/ψ plus jet production is a second viable tool to measure the polarized gluon distribution during Phase II of HERA-$\vec{N}$.

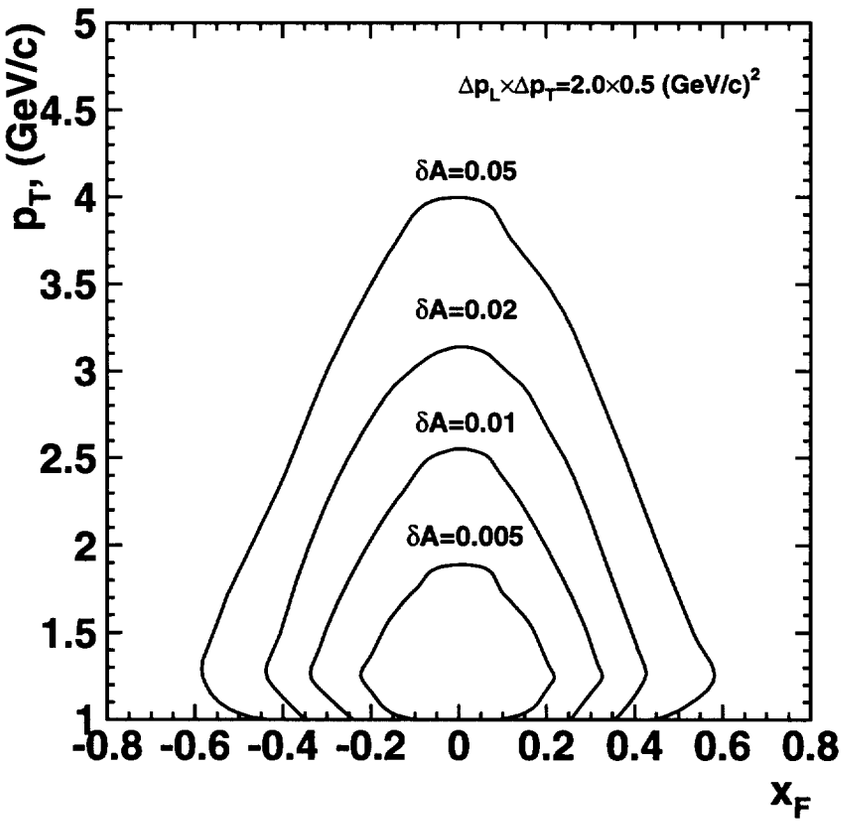

Figure 19: *Contours of the asymmetry sensitivity levels for $J/\psi \to e^+e^-$ production in the (p_T, x_F) plane.*

5.5 Λ and $\bar{\Lambda}$ Production

The longitudinal polarization of s or $\bar{s}$ quarks knocked out in hard scattering from the polarized target contains information about the spin-dependent parton distributions in the longitudinally polarized nucleon. The polarized outgoing $\bar{s}$- and s-quarks can be assumed to transmit its polarization with significant probability to $\bar{\Lambda}^0$ and Λ^0, respectively. The Λ-hyperon polarization can be easily measured in the weak self-analyzing decay

$$\Lambda^0(\bar{\Lambda}^0) \to p(\bar{p}) + \pi^-(\pi^+) \ . \tag{23}$$

Λ^0 and $\bar{\Lambda}^0$ hyperons produced in nucleon-nucleon scattering at 820 GeV beam energy have typical energies of $20 \div 40$ GeV. Due to their large life range ($c\tau = 7.89$ cm) they decay far from the target ($l = c\tau\gamma \sim 1.5 \div 3$ m). The angular distribution for the decay (23) in the $\Lambda(\bar{\Lambda})$ rest frame system can be described by

$$W = \frac{1}{4\pi}(1 + B\xi_\Lambda cos\theta_0) \ , \tag{24}$$

with $B = 0.642 \pm 0.013$ [60]. Here ξ_Λ denotes the transverse Λ^0-polarization and θ_0 is the angle between the proton momentum and the hyperon spin. Due to the large value of B in (24) it is quite feasible to determine the hyperon polarization measuring the decay angle distribution.

To describe the fragmentation processes for unpolarized particles we make use of PYTHIA 5.7 and JETSET 7.4 which give reasonable agreement with the experimental data. The polarization transfer from partons to $\bar{\Lambda}^0$ is accomplished as proposed in Ref. [61, 71]. The MC simulation allows to follow all chains of parton transformations to Λ^0. If Λ^0 contains the initial s-quark then its polarization ξ_{Λ^0} has been set equal to ξ_s - the s-quark polarization. In other words, the transfer coefficient C in the relation $\xi_{\Lambda^0} = C\ \xi_s$ is taken equal to 1. In specific models other values for C down to $\frac{1}{9}$ are proposed.
The cross section for $\bar{\Lambda}^0$ production was calculated taking into account the decay branching ratio and a Θ acceptance of $20 \div 300$ mrad for both decay particles. The dependence of the antihyperon polarization on the transverse momentum, $p_T^{\bar{\Lambda}}$, obtained in the framework of this approach, is presented in fig. 20 for different parametrizations of the polarized parton distributions [72, 73] and different schemes of the polarization transfer from partons to Λ [61, 71] which basically represent the region of predicted polarization values. As can be seen from the figure, the statistical errors attainable are reasonably small ($\lesssim 1\%$) up to $p_T \simeq 4$ GeV. In this region it is possible to distinguish between different model predictions.

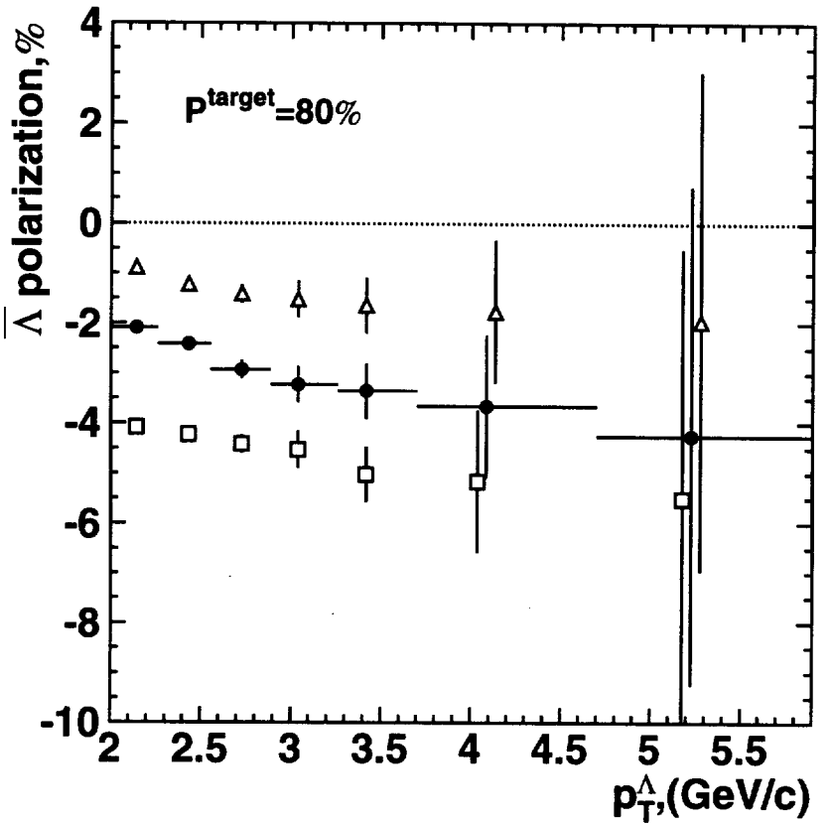

Figure 20: *Polarization of $\bar{\Lambda}^0$ as a function of p_T for different parametrizations of polarized parton distributions [72, 73] and different schemes of the polarization transfer from partons to Λ [61, 71].*

5.6 Elastic Scattering

Large unexpected spin effects in singly polarized proton-proton elastic scattering $p + p^{\uparrow} \rightarrow p + p$ have been discovered many years ago [74, 75] and remain unexplained up to now. The analysing power A_N was found significantly different from zero when the transverse momentum p_T of the scattered proton is large; A_N further increases with rising p_T^2, as shown later in fig. 22.

To illustrate the kinematics under HERA-$\vec{N}$ conditions the laboratory angles and momenta of the forward and recoil protons are shown in fig. 21 as a function of p_T^2. This figure clearly shows that the detection of the recoil proton for p_T^2 values in the range $5 \div 12$ $(\mathrm{GeV/c})^2$ requires a very large angular acceptance (up to 40 degrees) of the spectrometer. The forward protons for the same interval in p_T^2 have laboratory angles of the order of a few milliradians and require a dedicated detector very close to the beam pipe.
Note that although the probed p_t^2 range would be similar at HERA-$\vec{N}$ energies, it corresponds to protons with smaller angles to the collision axis in the CMS when comparing to existing data at lower energies.

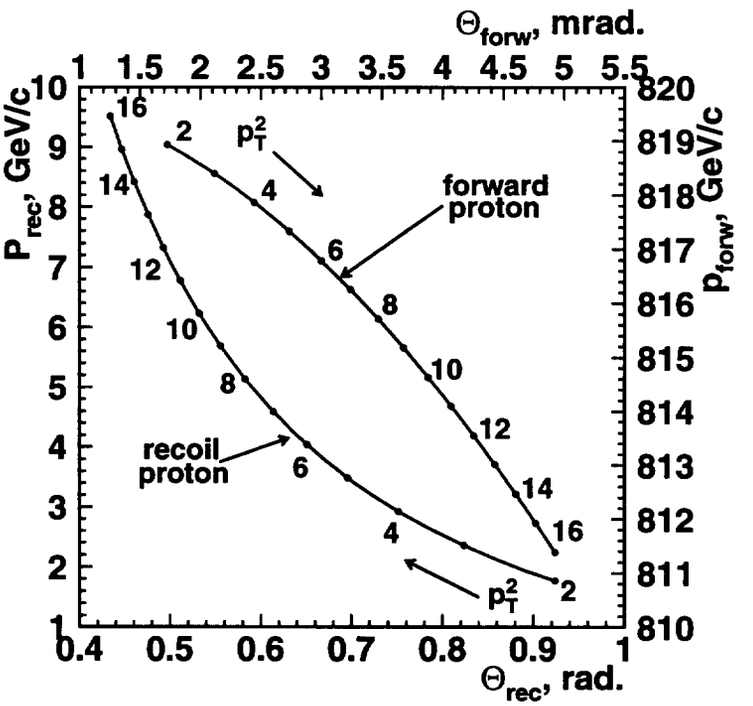

Figure 21: *Laboratory angles and momenta of the forward and recoil protons, respectively, for elastic proton-proton scattering as functions of* p_T^2.

To estimate the level of sensitivity δA_N in the left-right asymmetry A_N the differential cross section of proton-proton elastic scattering was taken in the form [76]:

$$\frac{d\sigma}{dt} = C \cdot t^{-8}, \quad C = 0.09\ mb \cdot GeV^{14}, \tag{25}$$

which is in good agreement with high energy data for $-t \gtrsim 3 \div 4$ $(\mathrm{GeV/c})^2$ at various Fermilab and ISR energies. It does not depend on the initial energy for beam energies above 300 GeV. The projected statistical error δA_N is displayed in fig. 22 as a function of p_t^2. We conclude that the existing data on singly polarized proton-proton elastic scattering can be checked with HERA-$\vec{N}$ in the region $5 \lesssim p_T^2 \lesssim 7$ $(\mathrm{GeV/c})^2$ with comparable accuracy. Moreover, some new data points up to $p_T^2 \simeq 10 \div 12$ $(\mathrm{GeV/c})^2$ can be measured. In this way it appears feasible to definitely clarify if the significant non-zero single spin asymmetries in elastic proton-proton scattering persist at those high energies.

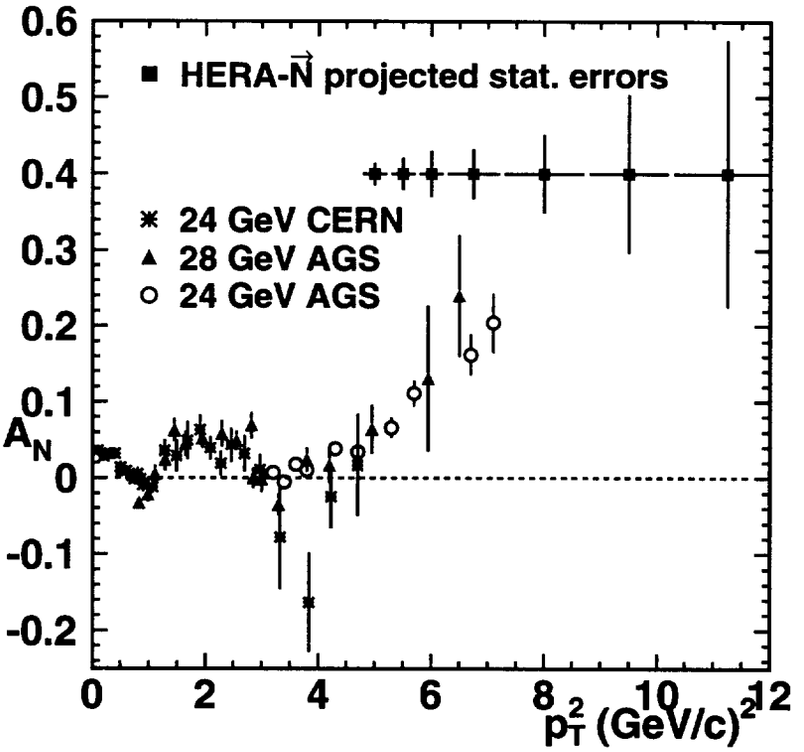

Figure 22: *Compilation of experimental data on the asymmetry in elastic proton-proton scattering as a function of p_T^2. CERN - Ref. [74], AGS - Ref. [75]. In addition the projected statistical errors attainable with HERA-$\vec{N}$ are shown.*

6 Conclusions

The physics reach was investigated of polarized nucleon-nucleon collisions originating from an internal target in the 820 GeV HERA proton beam. Single spin asymmetries, accessible already with the existing unpolarized beam, were found to be an almost unique and powerful tool to disentangle the QCD-inherent puzzle of multi-parton correlations in conjunction with results of other experiments at HERA. When measuring the polarized gluon distribution through various double spin asymmetries, requiring a polarized HERA proton beam, the projected statistical accuracies are found to be comparable to those predicted for the spin physics program at RHIC.

Acknowledgements

The results presented above were obtained during a several weeks workshop in Zeuthen which was made possible thanks to the generous support of DESY-IfH.
We are indebted to T. Gehrmann, G. Ladinsky and A. Schäfer for critical remarks and helpful comments.

References

[1] M. Göckeler, [15], p.339

[2] EMC, J. Ashman et al., *Phys. Lett. B 206*, 364 (1988)
EMC, J. Ashman et al., *Nucl. Phys. B 328*, 1 (1989)

[3] R. D. Ball, S. Forte, G. Ridolfi, *Nucl. Phys. B444*, 287 (1995);
CERN preprint TH/95-266, 1995

[4] E142 Coll., P. L. Anthony et al., *Phys. Rev. Lett. 71*, 959 (1993)

[5] E143 Coll., K. Abe et al., *Phys. Rev. Lett. 74*, 346 (1995)
E143 Coll., K. Abe et al., *Phys. Rev. Lett. 75*, 25 (1995)

[6] SMC, D. Adams et al., *Phys. Lett. B 329*, 399 (1994)

[7] E154 Coll., R. Arnold et al., *SLAC proposal E154*, 1993

[8] HERMES Coll., P. Green et al., HERMES Technical Design Report, *DESY-PRC 93/06*, July 1993

[9] E155 Coll., R. Arnold et al., *SLAC proposal E155*, 1993

[10] SMC, D. Adams et al., *Phys. Lett. B 336*, 125 (1994)

[11] E143 Coll., K. Abe et al., *Phys. Rev. Lett. 76*, 587 (1996)

[12] A. Schäfer et al., *Phys. Lett. B 321*, 121 (1994)

[13] SMC, B. Adeva et al., preprint CERN-PPE/95-187 (1995)

[14] G. Bunce et al., *Particle World 3*, 1 (1992)

[15] Proceedings of the *Workshop on the Prospects of Spin Physics at HERA*, Zeuthen, August 28-31, 1995, DESY 95–200, ed. by J.Blümlein and W.–D. Nowak

[16] HERA–B Coll., E. Hartouni et al., *HERA–B Design Report*, DESY-PRC 95/01, January 1995

[17] E. Steffens, K. Zapfe–Düren, [15], p.57

[18] Proceedings of the 2nd Meeting on *Possible Measurements of Singly Polarized $p\vec{p}$ and $p\vec{n}$ Collisions at HERA*, Zeuthen, Aug.31–Sept.2, 1995, Desy Zeuthen Internal Report 95-05, ed. by H. Böttcher and W.–D. Nowak

[19] W.–D. Nowak, [15], p.145

[20] S. B. Nurushev, [18], p. 3

[21] RSC Collaboration, *Proposal on Spin Physics using the RHIC Polarized Collider*, August 1992

[22] E704 Coll., D.L. Adams et al., *Phys. Lett. B 261*, 201 (1991)

[23] E704 Coll., D.L. Adams et al., *Phys. Lett. B 264*, 462 (1991)

[24] E704 Coll., D.L. Adams et al., *Phys. Lett. B 276*, 531 (1992)

[25] E704 Coll., D.L. Adams et al., *Z. Phys. C 56*, 181 (1992)

[26] D. Sivers, AIP Conference Proceedings 51, Particles and Fields Subseries, No. 17, *High Energy Physics with Polarized Beams and Polarized Targets*, Argonne, 1978, ed. by G. H. Thomas, p.505
D. Sivers, *Phys. Rev. D 41*, 83 (1990)

[27] D. Sivers, *Phys. Rev. D 41*, 261 (1991)

[28] J. Qiu, G. Sterman, Phys. Rev. Lett. 67, 2264 (1991)

[29] J. Collins, *Nucl. Phys. B 396*, 161 (1993)

[30] C. Boros, Liang Zuo-tang and Meng Ta-chung, *Phys. Rev. Lett. 70*, 1751 (1993)
C. Boros, Liang Zuo-tang and Meng Ta-chung, *Phys. Rev. D 51*, 4867 (1995)

[31] X. Artru, J. Czyzewski and H. Yabuki, preprint LYCEN/9423 and TPJU 12/94, May 1994, hep-ph/9405426

[32] M. Anselmino, M. Boglione and F. Murgia, Proceedings of the *XI International Symposium on High Energy Spin Physics*, Bloomington, Indiana, September 1994, p. 446

[33] A.V. Efremov, V.M. Korotkiyan and O.V. Teryaev, *Phys. Lett. B 348*, 577 (1995)

[34] M. Anselmino, M. Boglione, F. Murgia, *Phys. Lett. B 362*, 164 (1995)

[35] O. V. Teryaev, [15], p.132

[36] J.C. Collins, *Nucl. Phys. B 394*, 169 (1993)

[37] J.C. Collins, S.H. Heppelmann and G.A. Ladinsky, *Nucl. Phys. B 420*, 565 (1994)

[38] J. Szwed, *Phys. Lett. B 105*, 403 (1981)

[39] A.V. Efremov and O.V. Teryaev, *Yad. Fiz. 36* 242 (1982) [*Sov. J. Nucl. Phys. 36*, 140 (1982)]

[40] G. Kane, J. Pumplin and W. Repko, *Phys. Rev. Lett. 41*, 1698 (1978)

[41] A.P. Contogouris, B. Kamal, O. Korakianitis, F. Lebessis, Z. Merebashvili, *Nucl. Phys. Proc. Suppl. 39 BC*, 98 (1995)

[42] S. F. Heppelmann, Proceedings of *VII Lake Louise Winter Institute* , 1992, ed. by B. A. Campbell, A. N. Kamal, S. C. Khanna, L. G. Greenians, p.

[43] A. Yokosawa, AIP Conference Proceedings 343, *High Energy Spin Physics, 11th International Symposium*, Bloomington, Indiana, Sept. 1994, ed. by K. Heller and S. Smith, p. 841

[44] R.L. Jaffe, Xiang-dong Ji, *Nucl. Phys. B 375*, 527(1992)

[45] W.-D. Nowak, AIP Conference Proceedings 343, *High Energy Spin Physics, 11th International Symposium*, Bloomington, Indiana, Sept. 1994, ed. by K. Heller and S. Smith, p. 412

[46] T. Sjostrand, *Comput. Phys. Commun. 82*, 74 (1994)

[47] E704 Coll., D. L. Adams et al., *Phys.Lett. B345*, 569 (1995)

[48] S. Güllenstern, P. Gornicki, L. Mankiewicz, A. Schäfer, *Nucl. Phys. A560*, 494 (1993)

[49] S. Güllenstern, P. Gornicki, L. Mankiewicz, A. Schäfer, *Phys. Rev. D51*, 3305 (1995)

[50] S. Güllenstern, P. Gornicki, L. Mankiewicz, A. Schäfer, *Comput. Phys. Commun. 87*, 416 (1995)

[51] T. Gehrmann and W. J. Stirling, *Durham University preprint*, DTP/95/82, (1995).

[52] A. Yokosawa, talk at the Adriatico Research Conference on *Trends in Collider Spin Physics*, Trieste, Dec. 4-9, 1995

[53] G. Donaldson et al., *Phys. Lett. 73B*, 375 (1978)

[54] D. Drijard et al., *Nucl. Phys. B208*, 1 (1982)

[55] A. Breakstone et al., *Zeit. Phys. C69*, 55 (1995)

[56] M. Bourquin, J.-M. Gaillard, *Nucl. Phys. B114*, 334 (1976)

[57] J. Babcock, E. Monsay, D. Sivers, *Phys. Rev. D 19*, 1483 (1979)

[58] D. E. Jaffe et al., *Phys. Rev. D40*, 2777 (1989)

[59] A. Breakstone et al., *Phys. Lett. 135B*, 505 (1984)

[60] Particle Data Group, *Phys. Rev. D50*, 1173 (1994)

[61] G. Gustafson, J. Hakkinen, *Phys. Lett. B303*, 350 (1993)

[62] E.L. Berger and D. Jones, *Phys. Rev. D 23*, 1521 (1981)
R.Baier and R.Rückl, *Z. f. Phys. C 19*, 251 (1983)

[63] M.H. Schub et al., *Phys. Rev. D 52*,1307 (1995)

[64] F. Abe et al., *Phys. Rev. Lett. 69*, 3704 (1992)
F. Abe et al., *Phys. Rev. Lett. 71*,2537 (1993)
CDF Coll., K. Byrum, Proceedings of the *27th International Conference oh High Energy Physics*, Glasgow, (1994), eds. P.J. Bussey and I.G. Knowles (Inst. of Physics Publ.), p.989;

[65] G.T. Bodwin, E. Braaten, and G.P. Lepage, *Phys. Rev. D 51*, 1125 (1995)
E. Braaten ans S. Fleming, *Phys. Rev. Lett. 74*, 3327 (1995)
M. Cacciari, M. Greco, M.L. Mangano, and A. Petrelli, *Phys. Lett. B 356*,560 (1995)
P. Cho and A.K. Leibovich, CALT-68-1988 and CALT-68-2026

[66] H1 Collab., S. Aid et al., contribution to the *Int. Europhysics Conf. on High Energy Physics*, Brussels, 1995;

[67] M. Cacciari and M. Kramer, DESY 96-005;

[68] D. Kazakov et al., [18], p.43

[69] T. Morii, S. Tanaka, T. Yamanishi, *Phys. Lett. B 322*, 253 (1994)

[70] B. Pire, [18], p. 51
J.L. Cortes and B. Pire, *Phys. Rev. D 38*, 3586 (1988)

[71] A. A. Jgoun et al., [18], p.149

[72] S. Brodsky, M. Burkardt, I. Schmidt, *Nucl. Phys. B441*, 197 (1995)

[73] S. Keller, J. F. Owens, *Phys. Rev. D49*, 1999 (1991)

[74] J. Antille et al., *Nucl. Phys. B185*, 1 (1981)

[75] D. G. Crabb et al., *Nucl. Phys. B121*, 231 (1977)
P. H. Hansen et al., *Phys. Rev. Lett. 50*, 802 (1983)
D. C. Peaslee et al., *Phys. Rev. Lett. 51*, 2359 (1983)
P. R. Cameron et al., *Phys. Rev. D 32*, 3070 (1985)
D. G. Crabb et al., *Phys. Rev. Lett. 65*, 3241 (1990)

[76] M. Jacob, P. V. Landshoff, *Phys.Rep. 48*, 285 (1978)